STAR Results in the Upcoming EIC Era

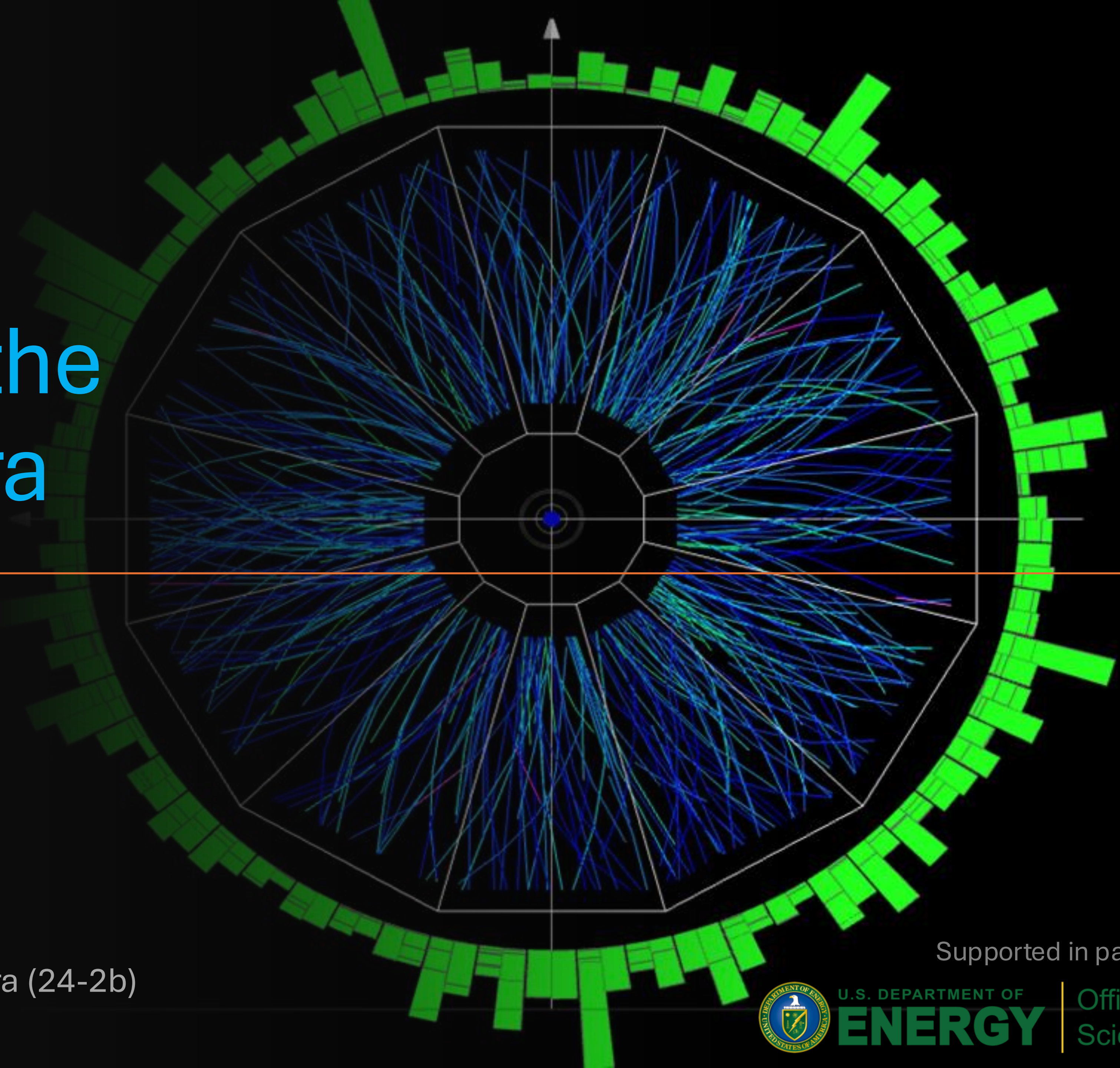

Grigory Nigmatkulov
(for the STAR experiment)
University of Illinois Chicago

INT program: Heavy Ion Physics in the EIC Era (24-2b)
Seattle, WA August 19 – August 24, 2024

Supported in part by
U.S. DEPARTMENT OF ENERGY | Office of Science

Outline

- J/ψ production in ultraperipheral collisions
- Vector meson spin interference
- Baryon number carrier and its transport
- EM-jet A_N studies at 200 GeV
- Nonlinear gluon effects in QCD

J/ψ production in ultraperipheral collisions

The strongest EM-fields in UPCs

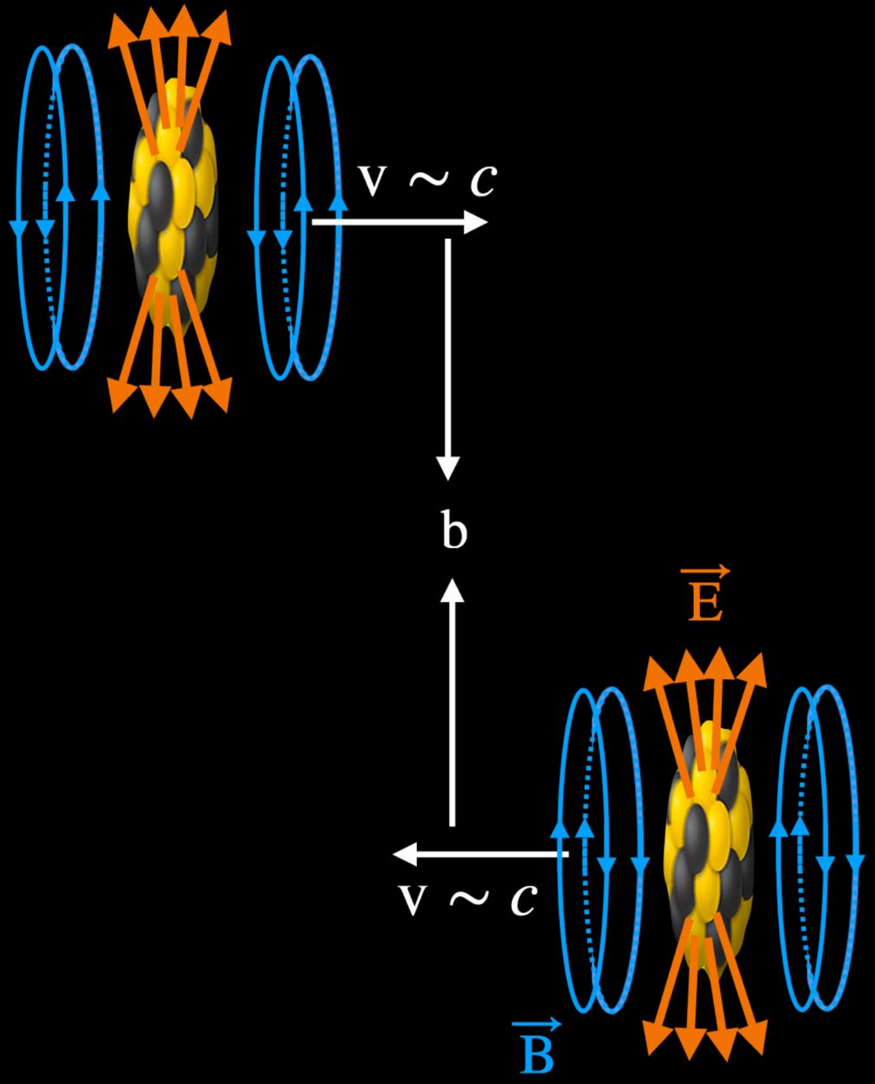

- In UPCs,

  $E_{max} = 10^{18}$ V/m , $B_{max} \sim 10^{14} - 10^{18}$ T

  => Strongest EM-field in the universe, but transient

- EM-field treated in terms of quasi-real photons

  $W_{\gamma,max} \sim \gamma\hbar c/R$;

  $W_{\gamma,max} \sim 3$ GeV (RHIC)

  $W_{\gamma,max} \sim 80$ GeV (LHC)

=> EM-fields are quantized as photons in UPCs

Photon-gluon scattering

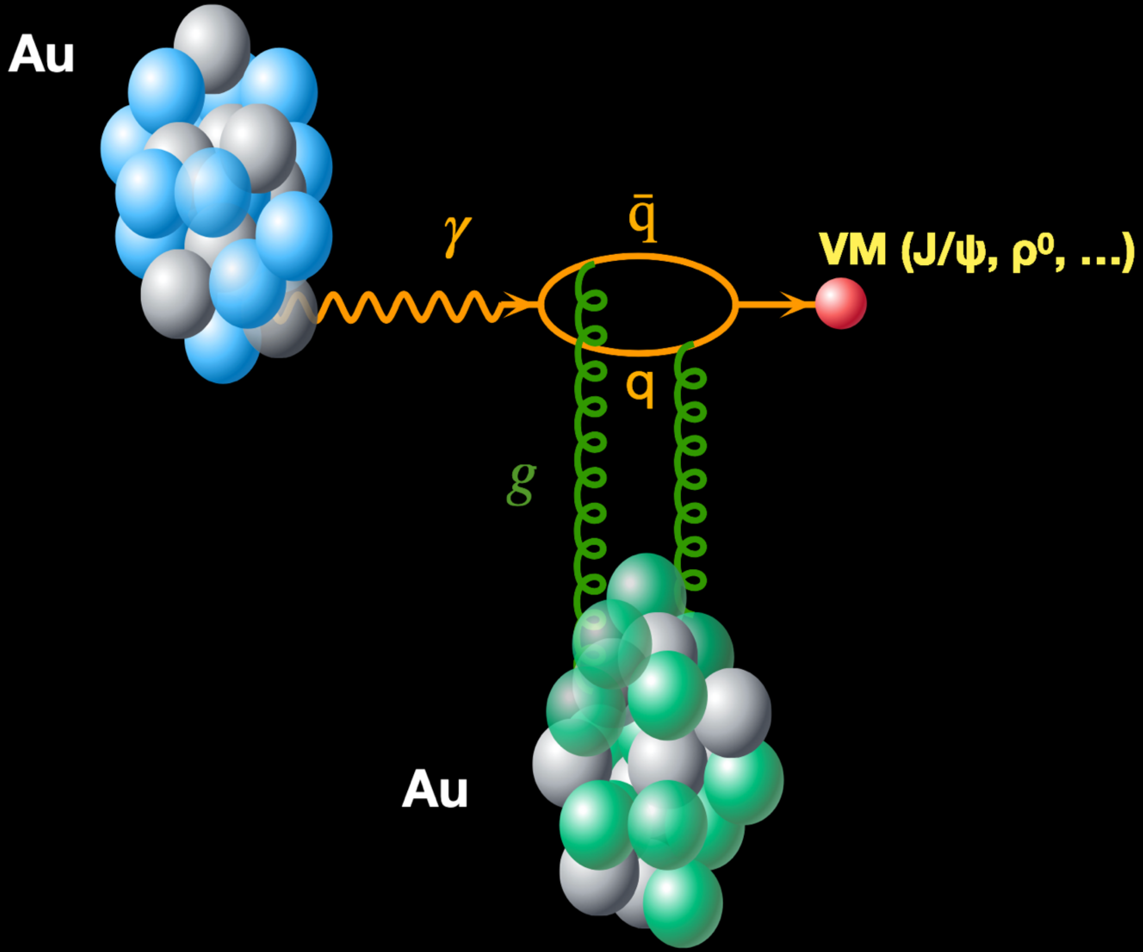

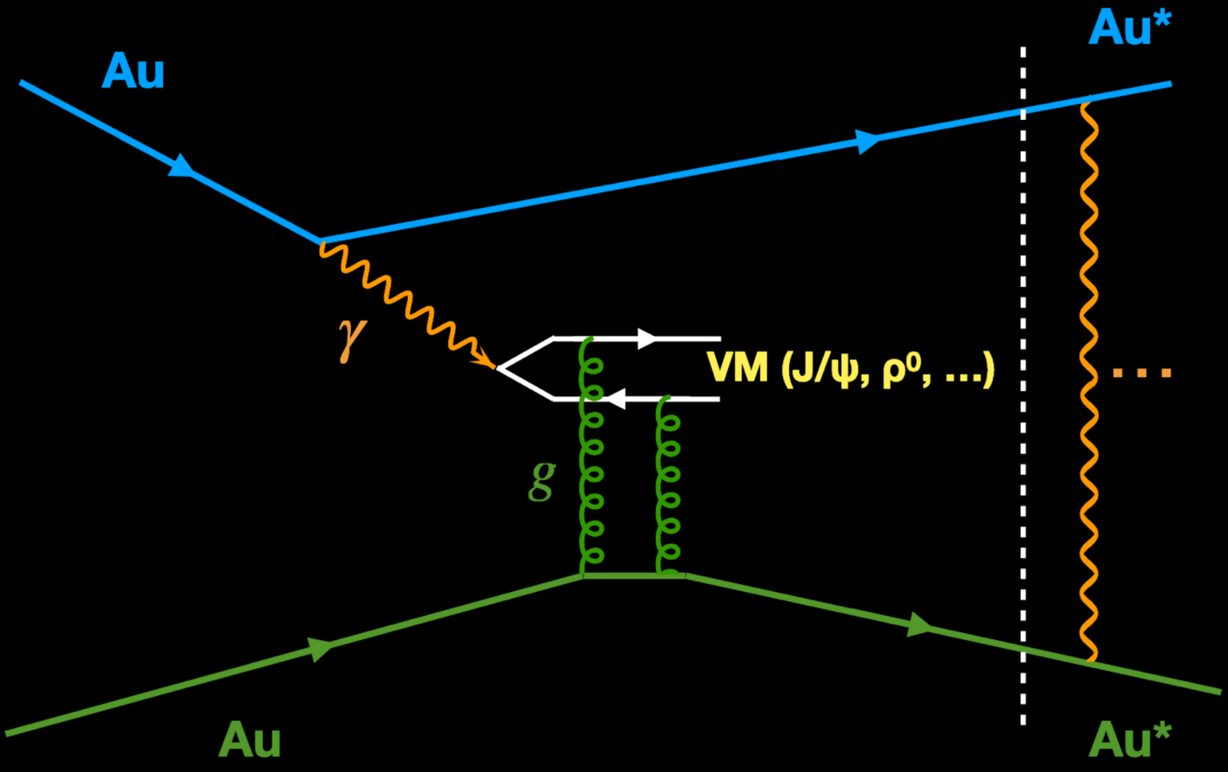

fig: Ashik Ikbal, RHIC-AGS 2024

Photoproduction of Vector Mesons (VM) in UPC

UPC VM: Powerful probe of parton densities inside nuclei

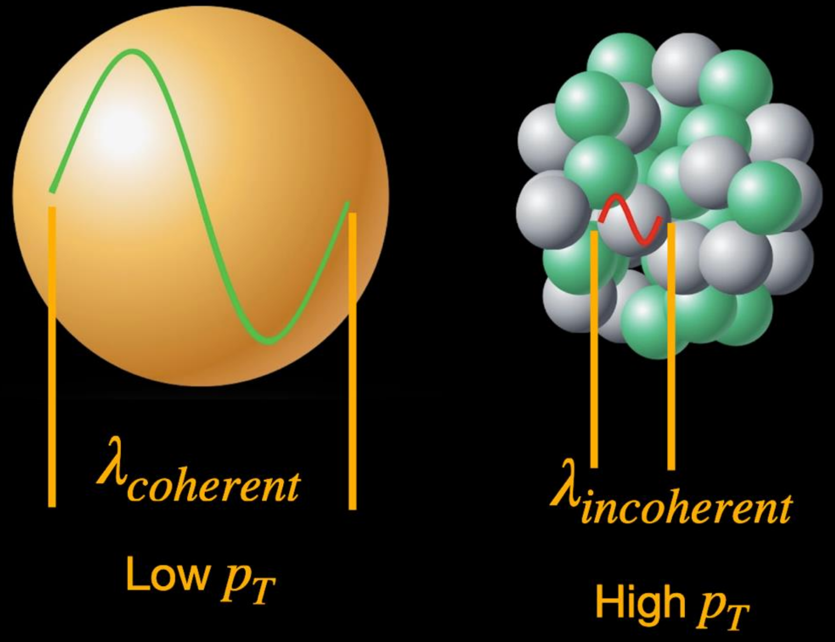

Satre simulation of parton density fluctuations, Fig: A. Kumar

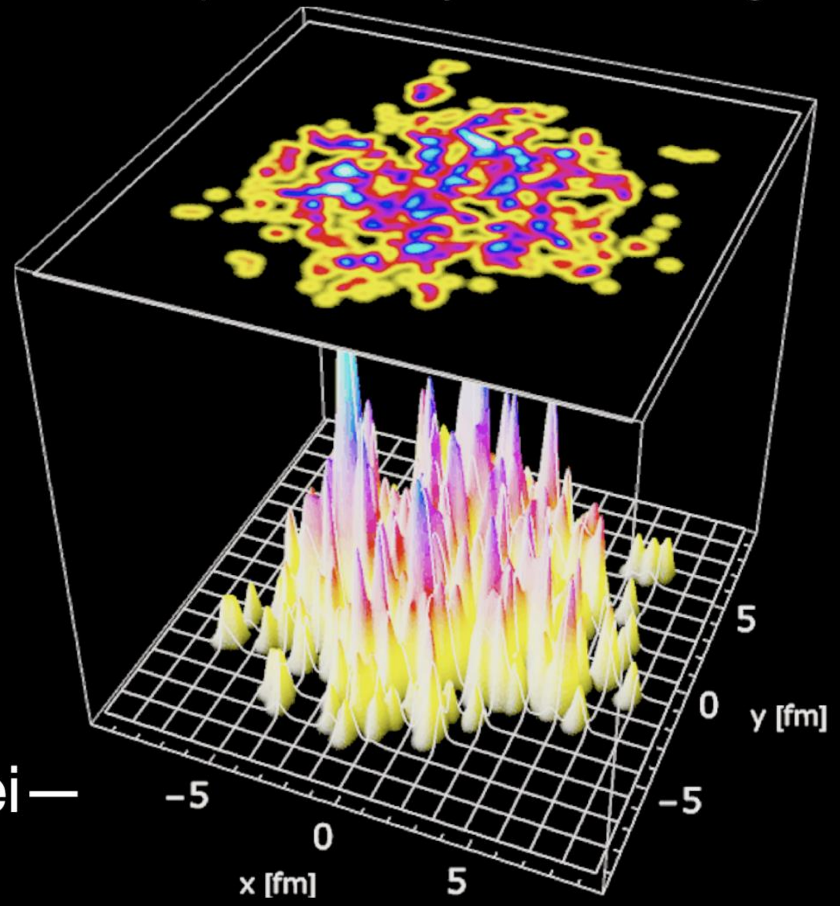

- ◉ Probes parton density & fluctuations inside nuclei— constraints for A+A initial state
- ◉ Modification of parton densities in heavy nuclei

=> VMs help to probe parton density inside nuclei before EIC era

UPC events with STAR detector

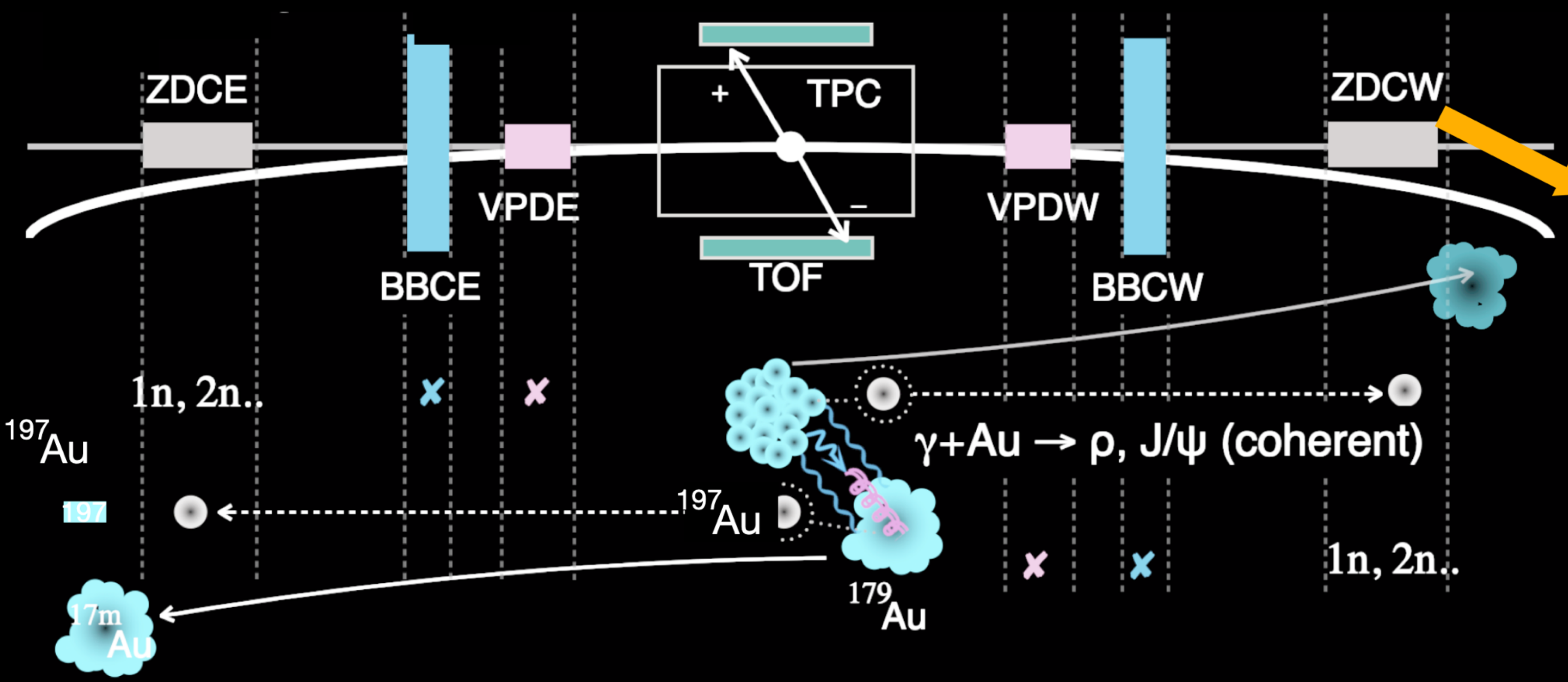

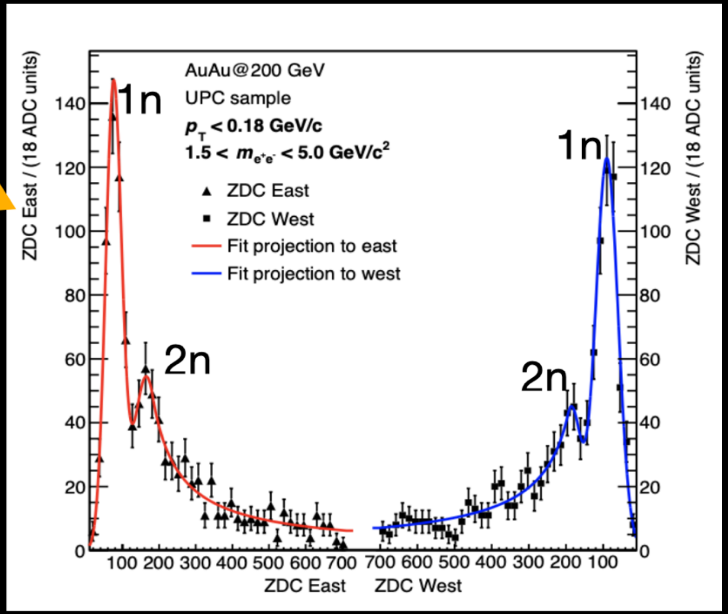

- Neutron(s) detected in ZDCs
- ZDC signals show peak structure for neutrons
- No activity in both BBCs => Diffractive events (η-gap)

=> Method to trigger UPC events

J/ψ measurements in 200 GeV Au+Au UPCs

STAR, PRC 110 (2024) 014911

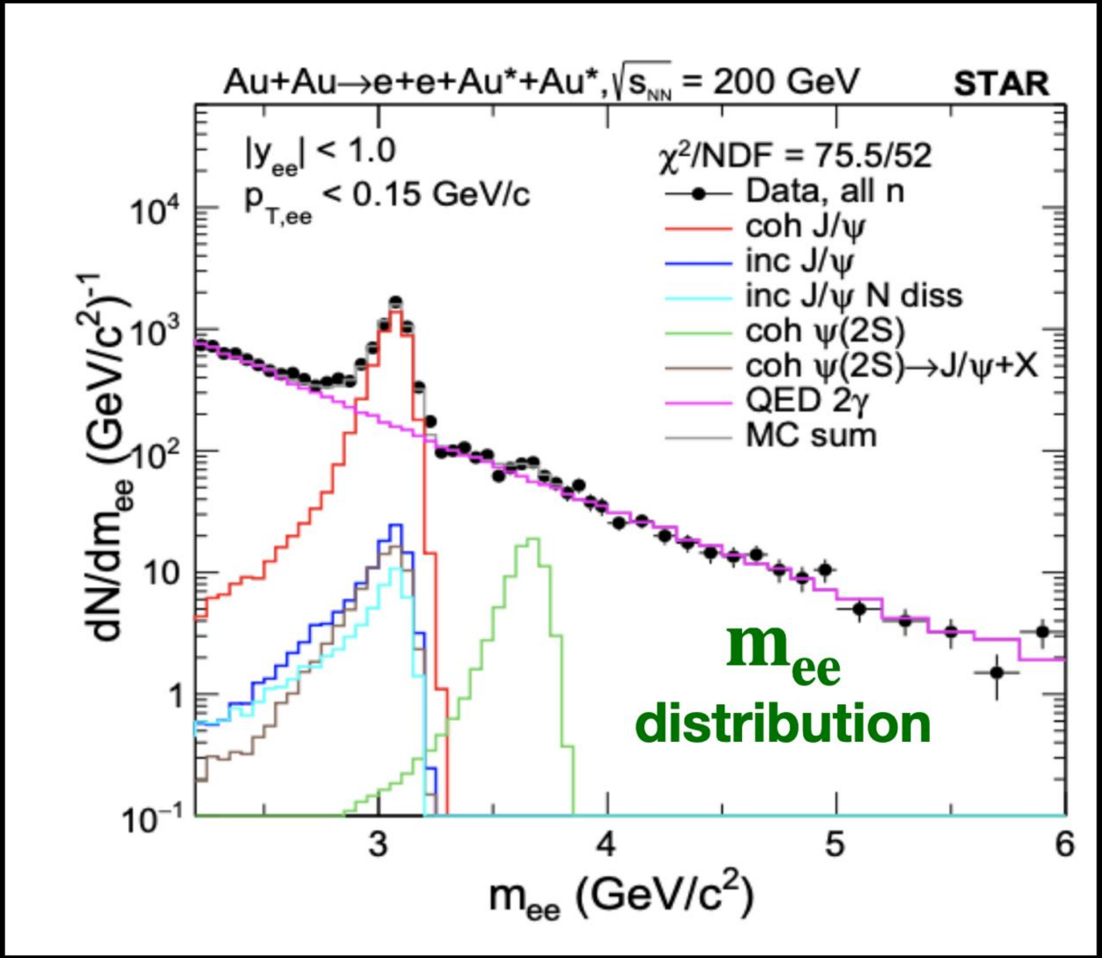

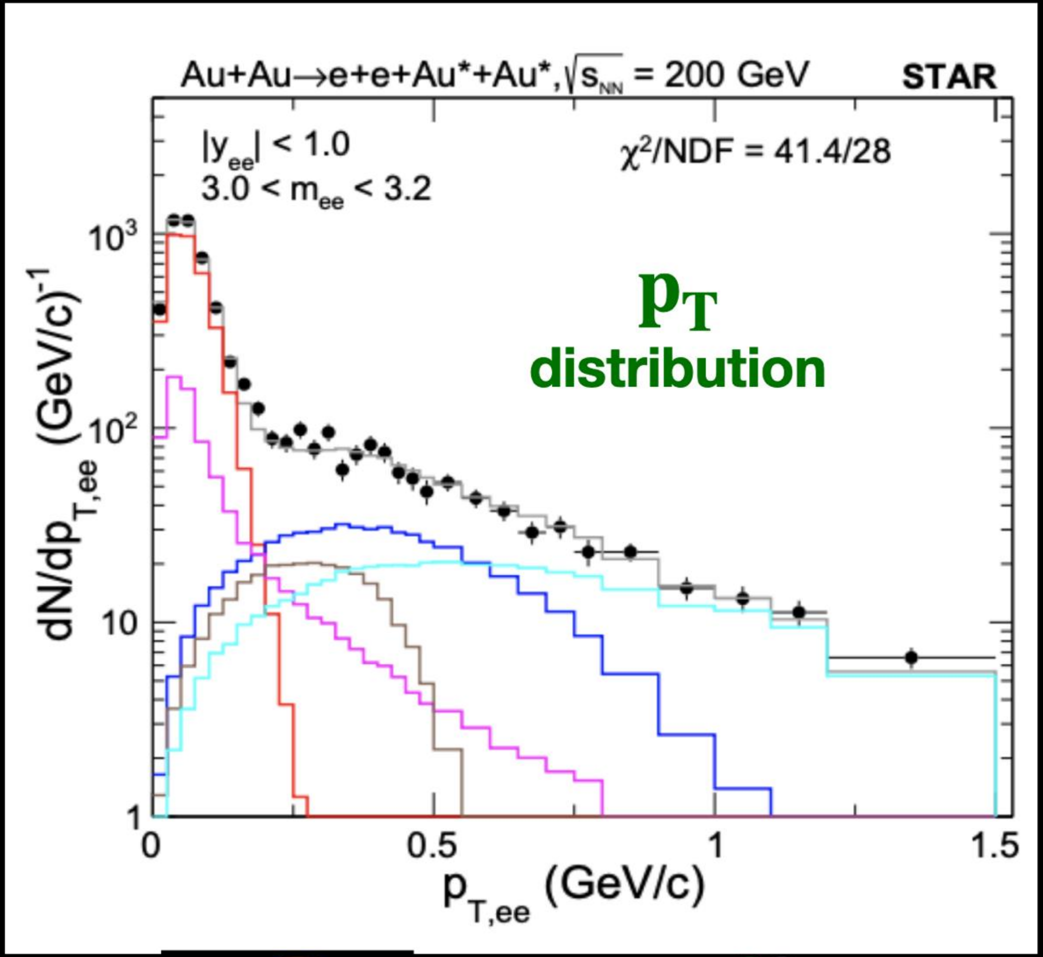

=> Coherent and incoherent contributions can be disentangled via the combined fit of mass and p_T

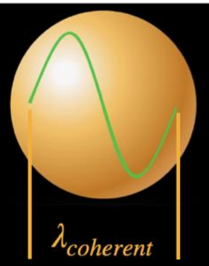

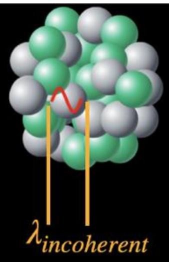

Rapidity dependence J/ψ production cross-section

STAR, arXiv:2311.13637

- Measured for coherent and incoherent contributions for different neutron emission in ZDCs
- Systematic unc. in incoherent to coherent cross-section ratio are largely cancelled
- Sensitive to the nuclear structure and deformation

=> Important to constrain theoretical models related to nuclear geometry

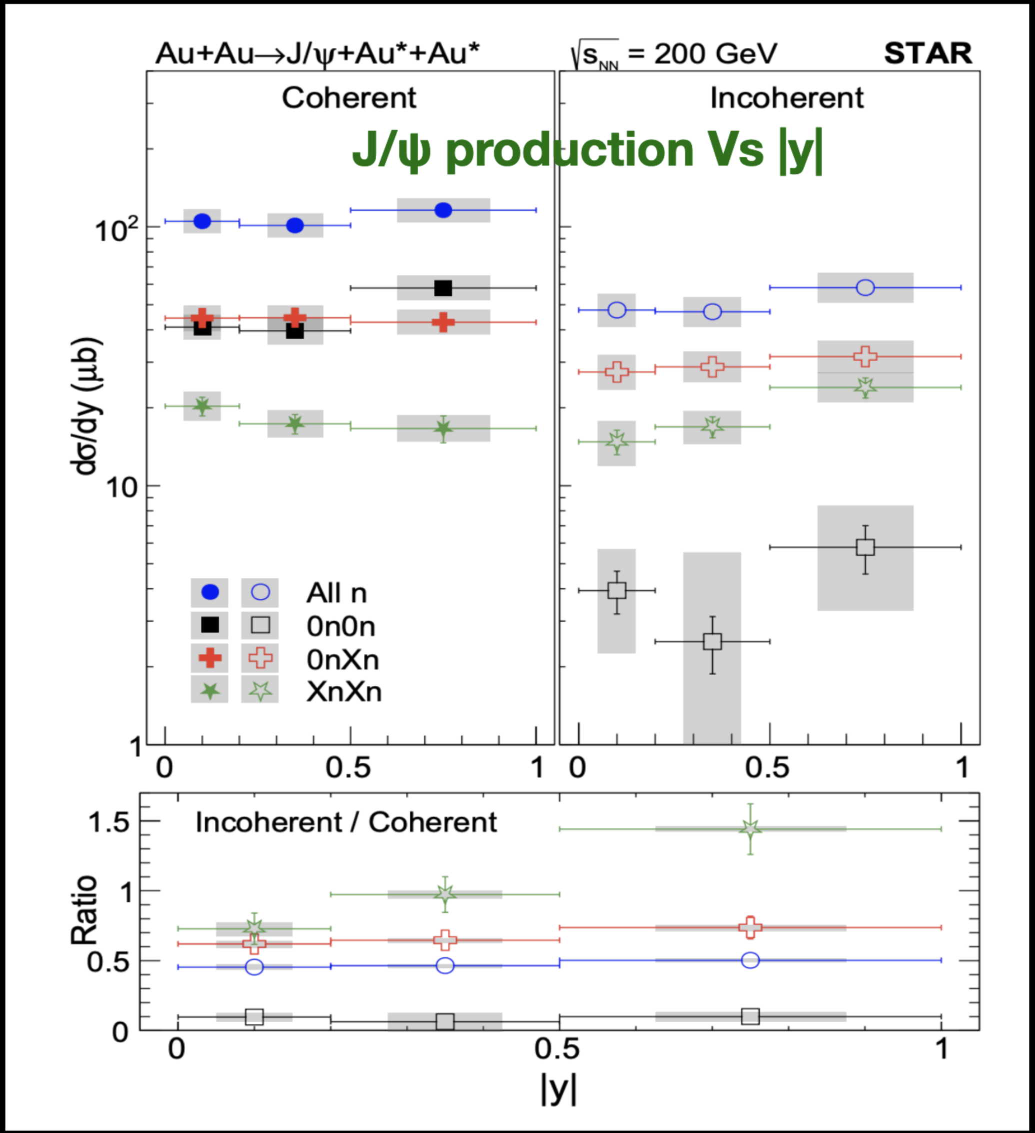

Incoherent J/ψ production cross-section vs p_T^2

STAR, arXiv:2311.13632

- Incoherent production compared with H1 data with free proton
- Strong nuclear suppression (~49%) seen
  (Mäntysaari et. al, Phys. Rev. Lett. **117** (2016) 5, 052301)
- Models found H1 data supports sub-nucleonic fluctuations
  (Mäntysaari et. al, Phys. Rev. D **106** (2022) 7, 074019)
- STAR data shows the bound nucleon has similar shape as the free proton — similar sub-nucleonic fluctuations in heavy nuclei

=> Strong nuclear suppression and sub-nucleonic fluctuations in Au nucleus

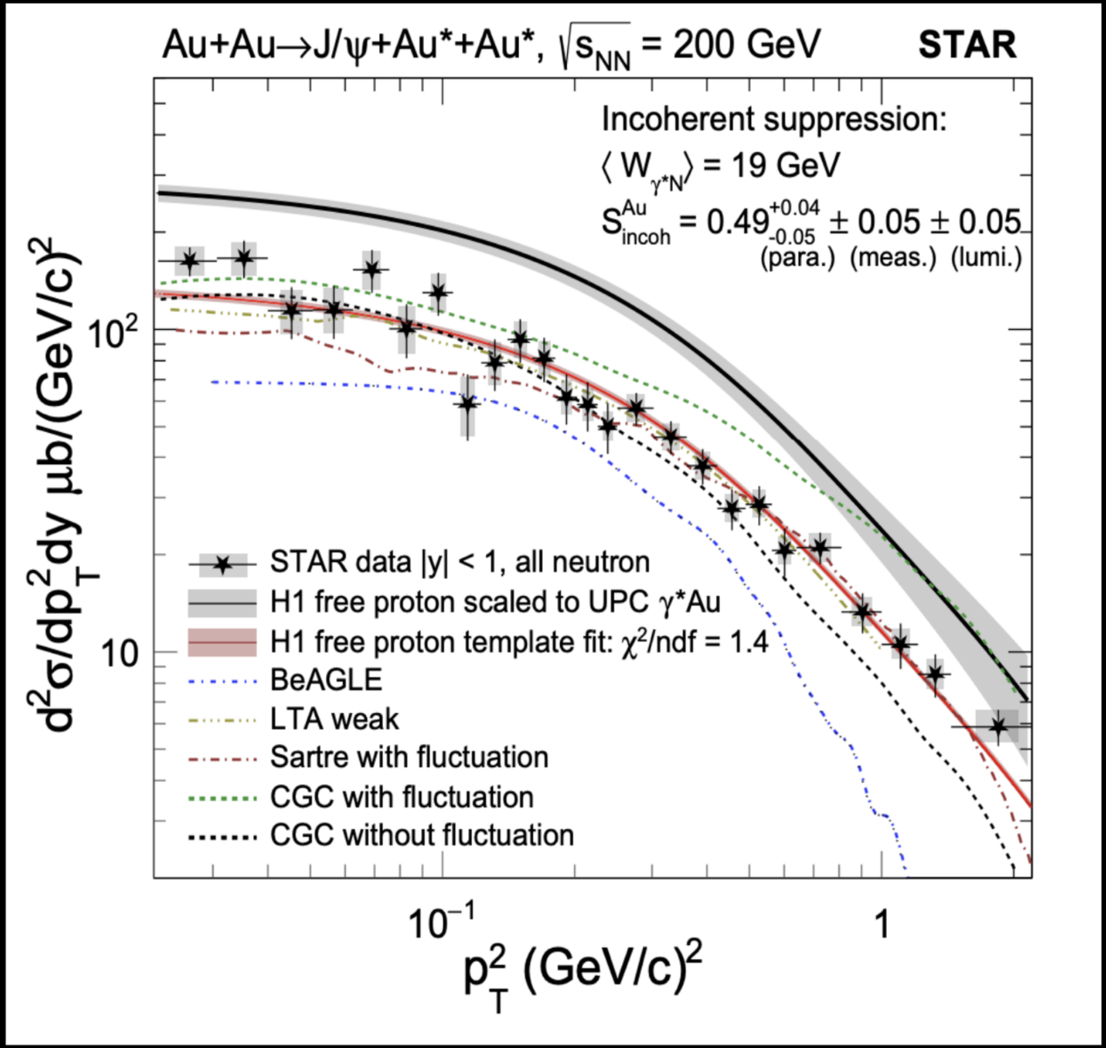

Vector meson spin interference

Polarized Photons from colliding nuclei

STAR, Phys. Rev. Lett. 127 (2021) 52302

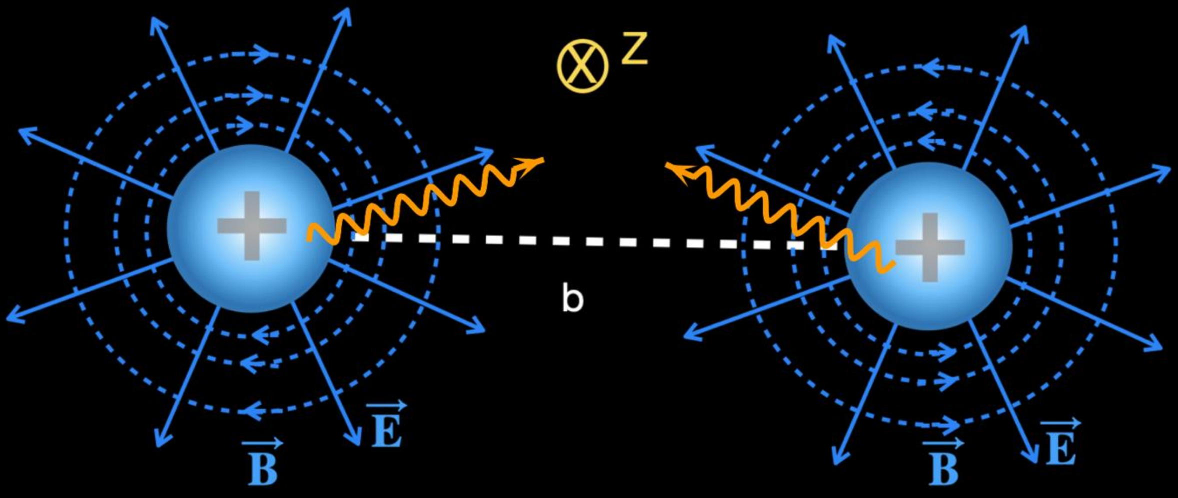

Transverse view of Lorentz contracted nuclei

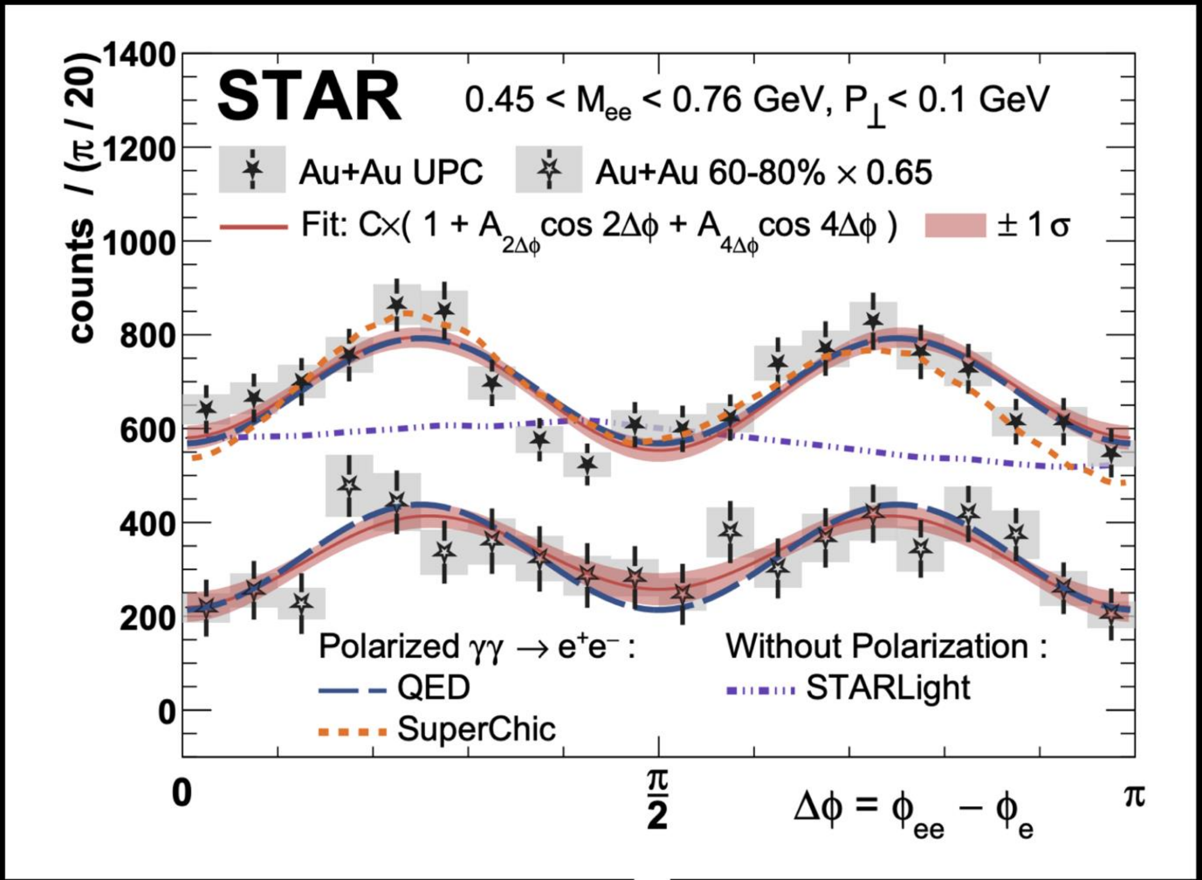

=> Photons in UPC are linearly polarized

Experimental access to photon polarization demonstrated by STAR, measuring the Breit-Wheeler process, $\gamma\gamma \rightarrow e^+e^-$

UPC vector meson spin and decay daughters are correlated

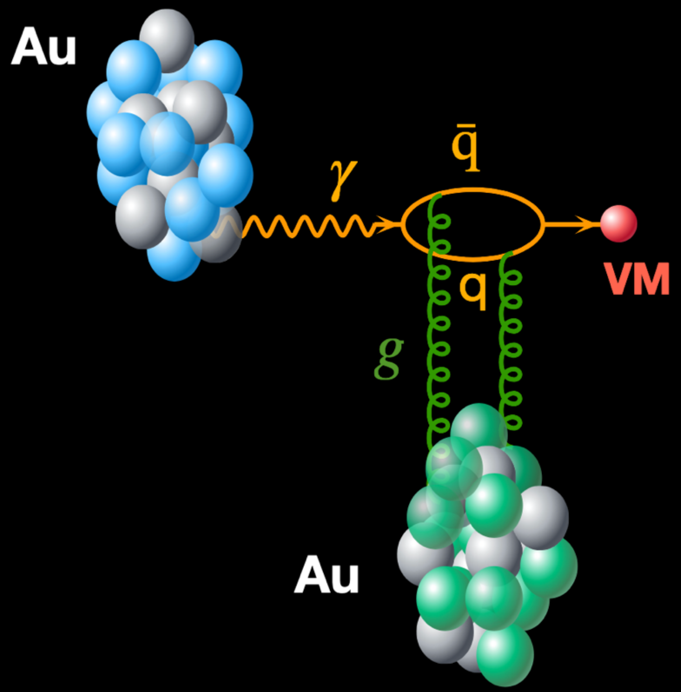

fig: Ashik Ikbal, RHIC-AGS 2024

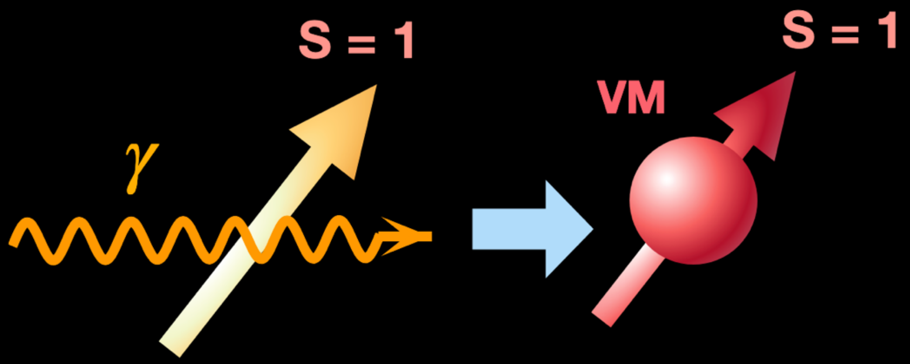

Polarization of photon
→ Inherited by VM

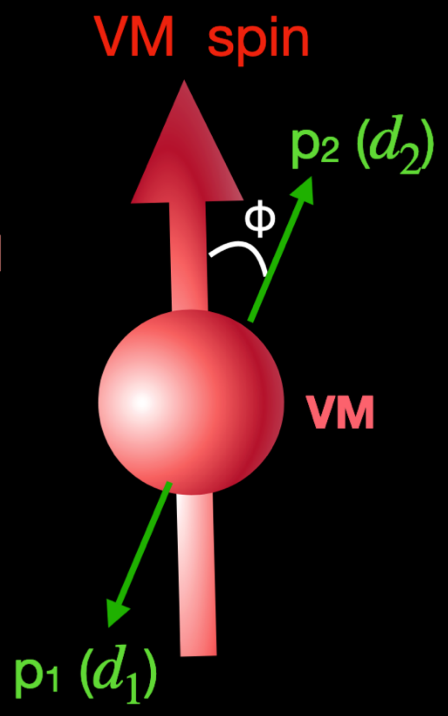

Decay VM → $d_1 d_2$ daughters preferentially emitted (L+S conservation)

=> The cos(2ϕ) modulation in VM momentum distribution w.r.t photon polarization direction

Measuring the modulation over a large no. of events

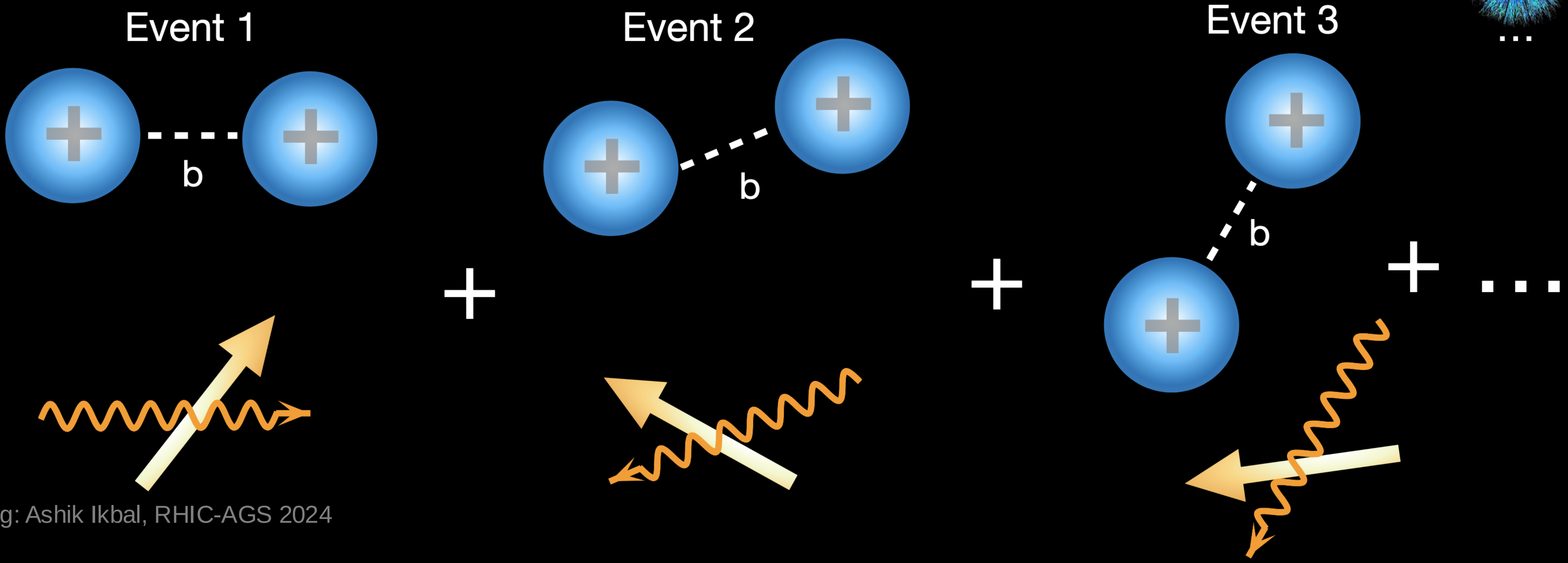

fig: Ashik Ikbal, RHIC-AGS 2024

Photon polarization correlated with Impact parameter —> random from one event to the next

=> Event average washes out the cos(2ϕ) modulation w.r.t photon polarization direction

Interference makes the modulation observable in experiment

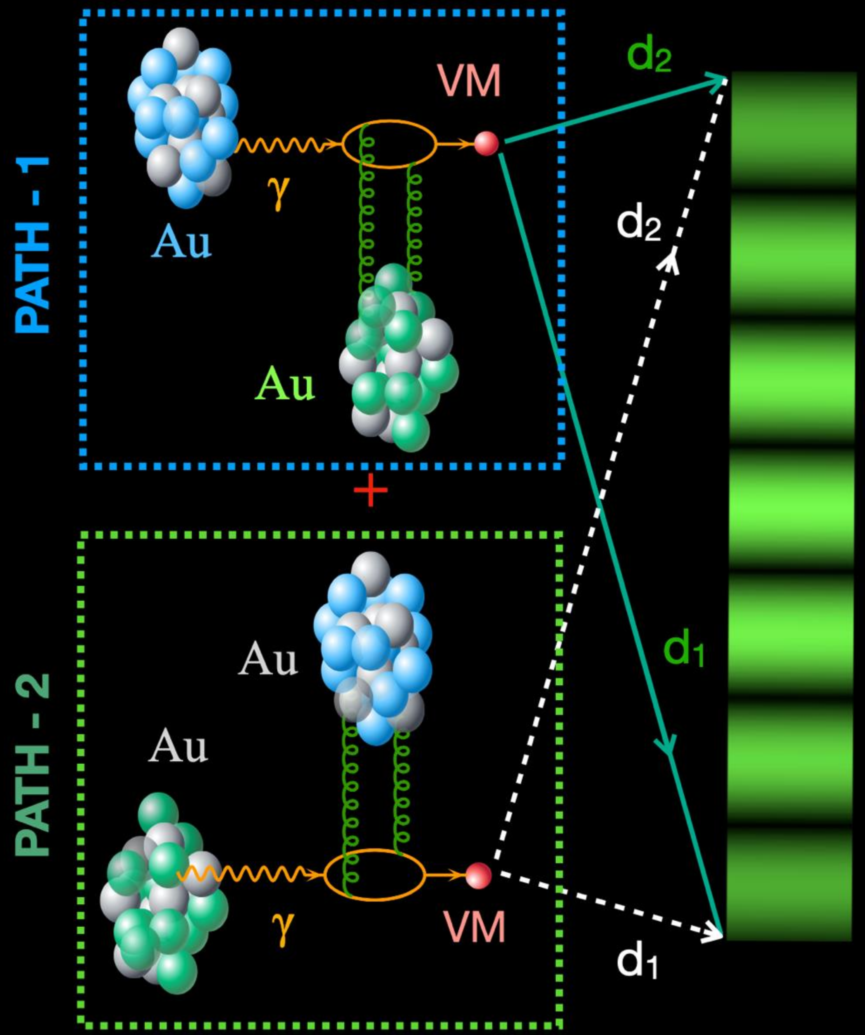

Photon source ambiguity: Interference among amplitudes of two possible paths

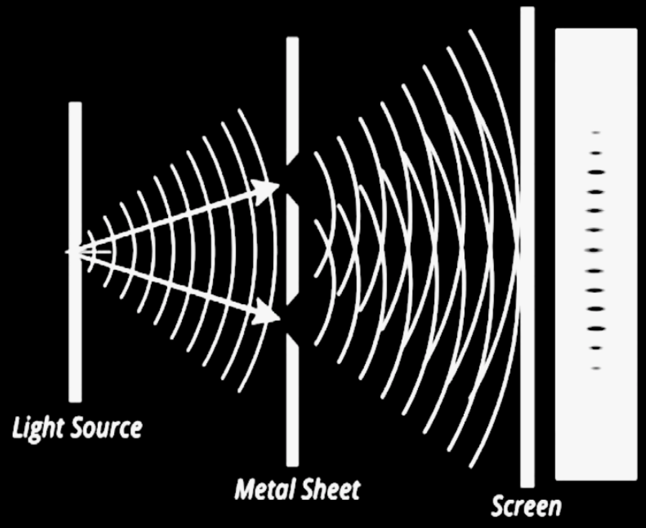

Double Slit Experiment

Best analogy: Double slit experiment in Optics

=> Two indistinguishable paths may interfere and make the cos(2ϕ) modulation observable

Observation of interference for $\rho^0 \to \pi^+\pi^-$ at STAR

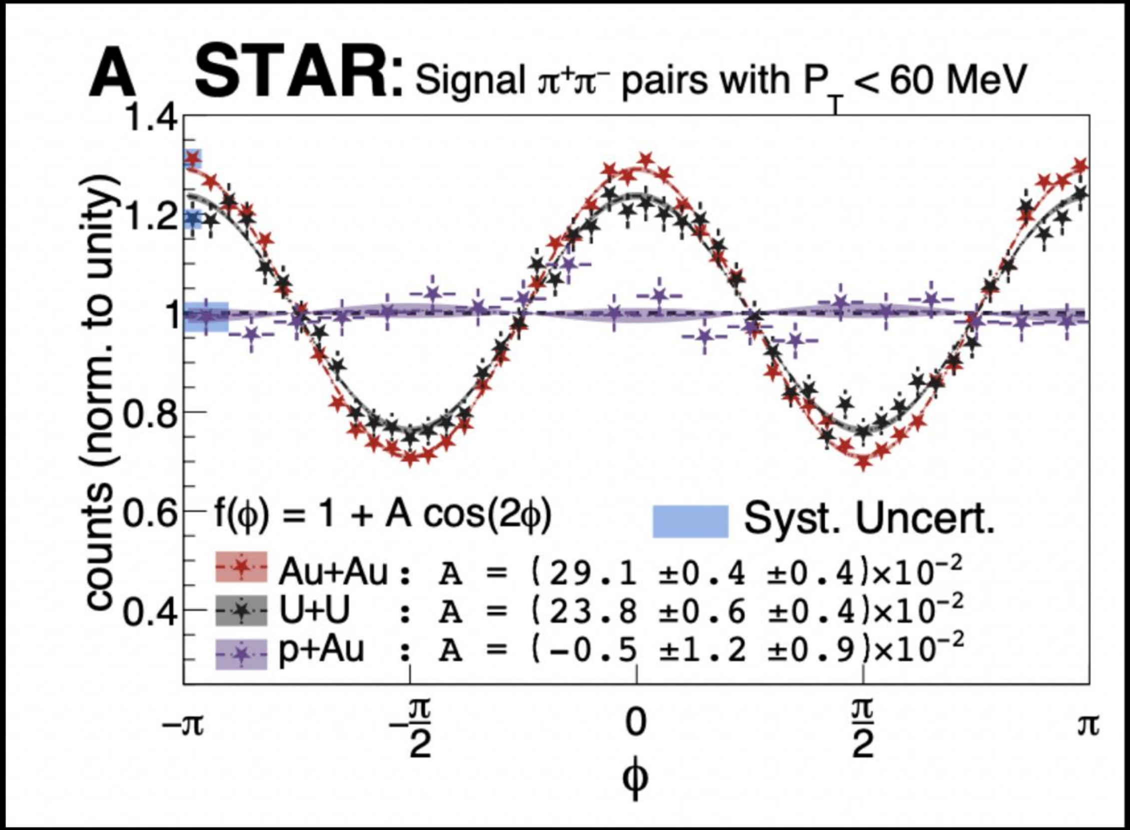

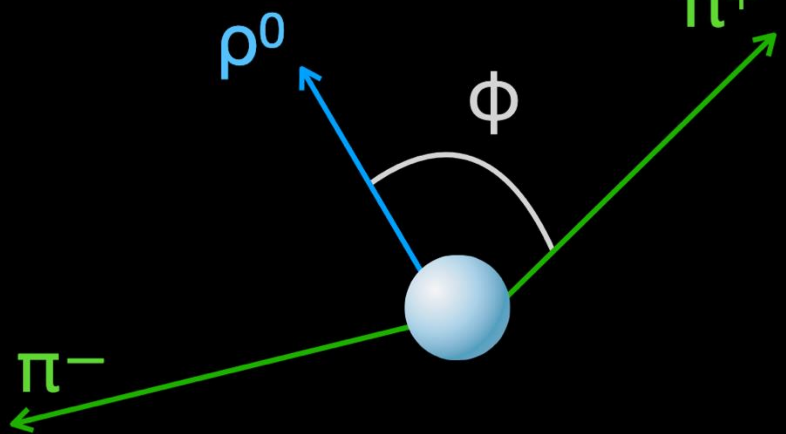

SCIENCE ADVANCES | RESEARCH ARTICLE

PHYSICS **STAR, Sci. Adv. 9, eabq 3903 (2023)**

Tomography of ultrarelativistic nuclei with polarized photon-gluon collisions

STAR Collaboration

A linearly polarized photon can be quantized from the Lorentz-boosted electromagnetic field of a nucleus traveling at ultrarelativistic speed. When two relativistic heavy nuclei pass one another at a distance of a few nuclear radii, the photon from one nucleus may interact through a virtual quark-antiquark pair with gluons from the other nucleus, forming a short-lived vector meson (e.g., ρ^0). In this experiment, the polarization was used in diffractive photoproduction to observe a unique spin interference pattern in the angular distribution of $\rho^0 \to \pi^+\pi^-$ decays. The observed interference is a result of an overlap of two wave functions at a distance an order of magnitude larger than the ρ^0 travel distance within its lifetime. The strong-interaction nuclear radii were extracted from these diffractive interactions and found to be 6.53 ± 0.06 fm (^{197}Au) and 7.29 ± 0.08 fm (^{238}U), larger than the nuclear charge radii. The observable is demonstrated to be sensitive to the nuclear geometry and quantum interference of nonidentical particles.

STAR, Sci. Adv. 9, eabq 3903 (2023)

Observed the interference for coherent ρ^0 photoproduction in UPCs

Measured in 3 different collision systems: Au+Au, U+U, p+Au —> Sensitive to nuclear shape/size

The p_T dependence of interference for $\rho^0 \rightarrow \pi^+\pi^-$ at STAR

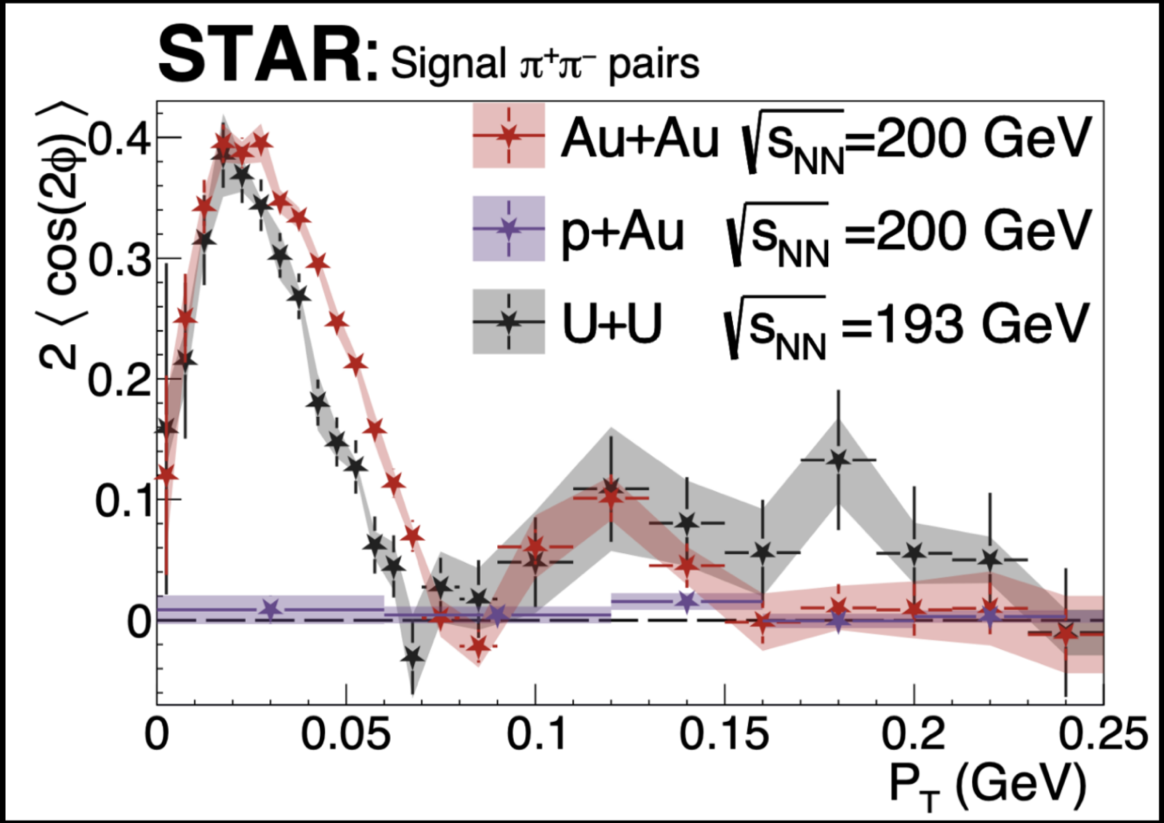

STAR, Sci. Adv. 9, eabq 3903 (2023)

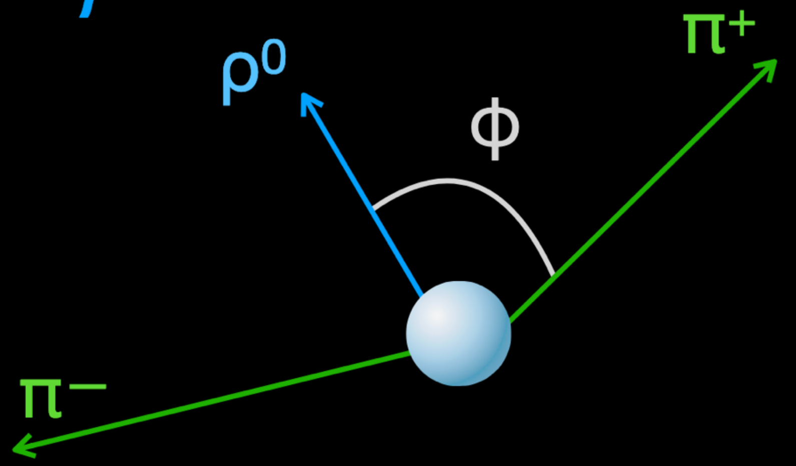

SCIENCE ADVANCES | RESEARCH ARTICLE

PHYSICS STAR, Sci. Adv. 9, eabq 3903 (2023)

Tomography of ultrarelativistic nuclei with polarized photon-gluon collisions

STAR Collaboration

A linearly polarized photon can be quantized from the Lorentz-boosted electromagnetic field of a nucleus traveling at ultrarelativistic speed. When two relativistic heavy nuclei pass one another at a distance of a few nuclear radii, the photon from one nucleus may interact through a virtual quark-antiquark pair with gluons from the other nucleus, forming a short-lived vector meson (e.g., ρ^0). In this experiment, the polarization was used in diffractive photoproduction to observe a unique spin interference pattern in the angular distribution of $\rho^0 \rightarrow \pi^+\pi^-$ decays. The observed interference is a result of an overlap of two wave functions at a distance an order of magnitude larger than the ρ^0 travel distance within its lifetime. The strong-interaction nuclear radii were extracted from these diffractive interactions and found to be 6.53 ± 0.06 fm (^{197}Au) and 7.29 ± 0.08 fm (^{238}U), larger than the nuclear charge radii. The observable is demonstrated to be sensitive to the nuclear geometry and quantum interference of nonidentical particles.

Clear p_T dependence of interference observed

Interference gets weak at higher p_T —
Incoherent processes take over

Radius measurement with interference for $\rho^0 \to \pi^+\pi^-$ at STAR

STAR, Sci. Adv. 9, eabq 3903 (2023)

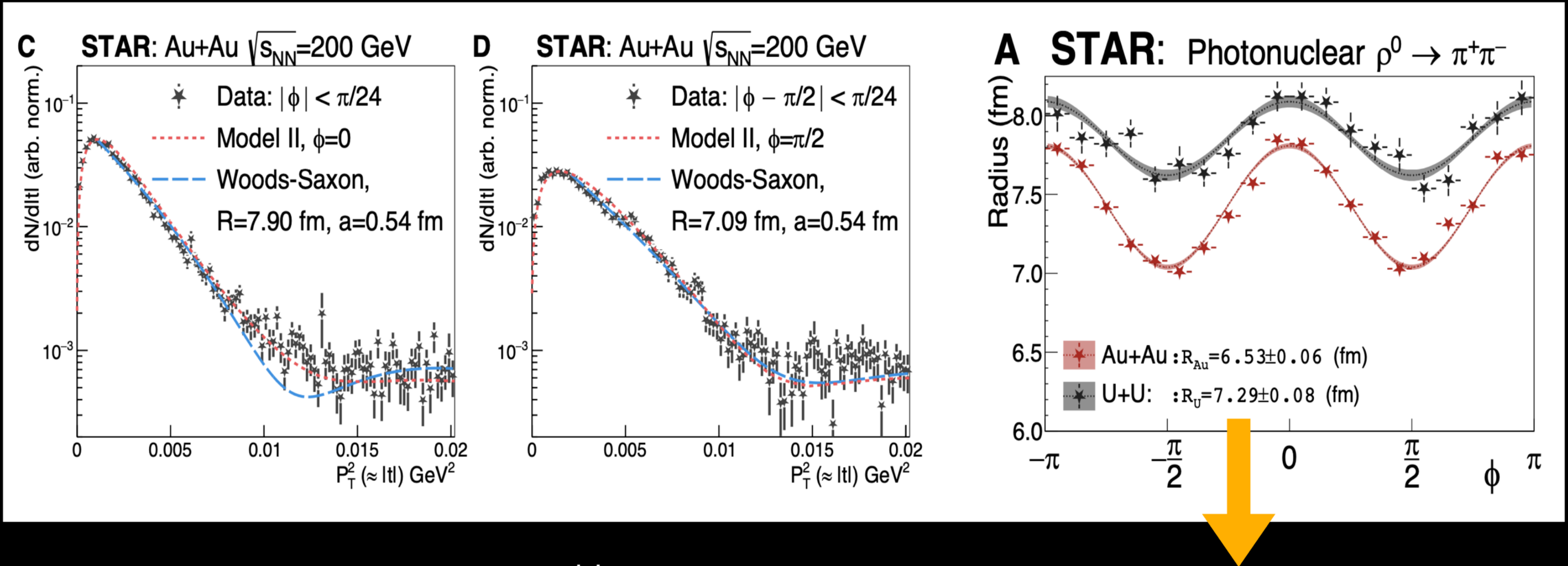

Impact of spin interference on |t| distribution studied in different ϕ bins

Improved measurement of mass radii using spin interference effect

R (Au) = 6.53 ± 06 fm; R (U) = 7.29 ± 08 fm

Spin interference with J/ψ $\rightarrow e^+e^-$

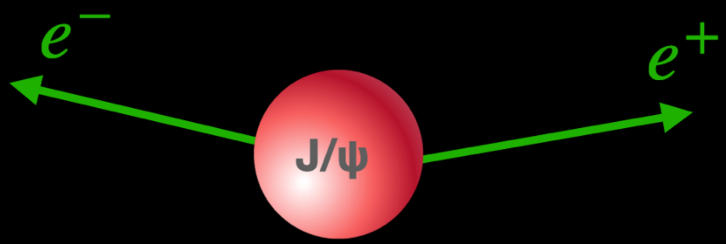

J/ψ $\rightarrow e^+e^-$

Boson Fermions

Mass: 0.7 GeV/c^2
Lifetime: 1.3 fm/c

Mass: 3.1 GeV/c^2
Lifetime: 2160 fm/c

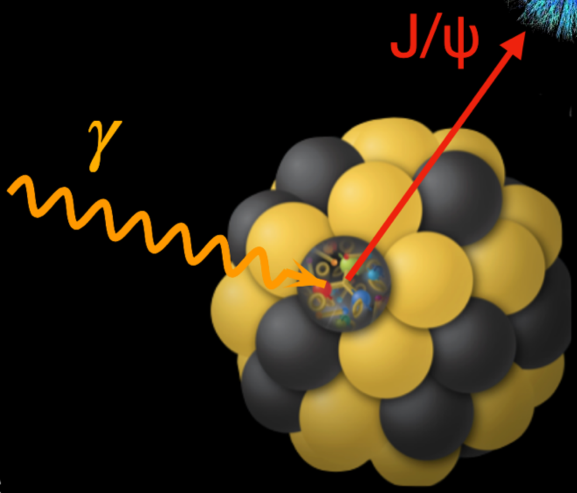

Measured sign of the interference tells us the level of interference

Interference of quantum particles —> Spin interference

—> J/ψ heavier than ρ^0 and J/ψ has much longer lifetime

—> J/ψ decay length much longer than typical distance b/w two colliding nuclei in UPCs

—> Probes finer structure and captures high quality images of the gluon distributions

Measured spin interference with J/ψ → e^+e^-

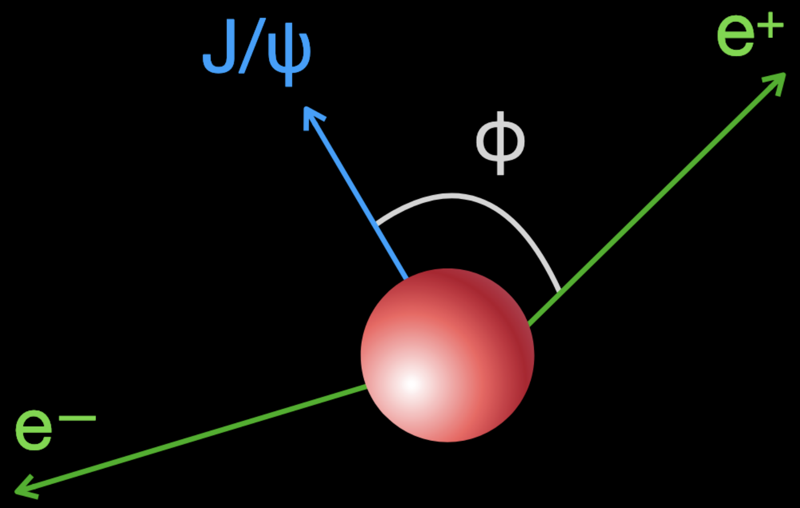

Observable for J/ψ spin interference

Interference signal fitted with: 1+ a_2 cos(2ϕ) => a_2 is the measure of the modulation

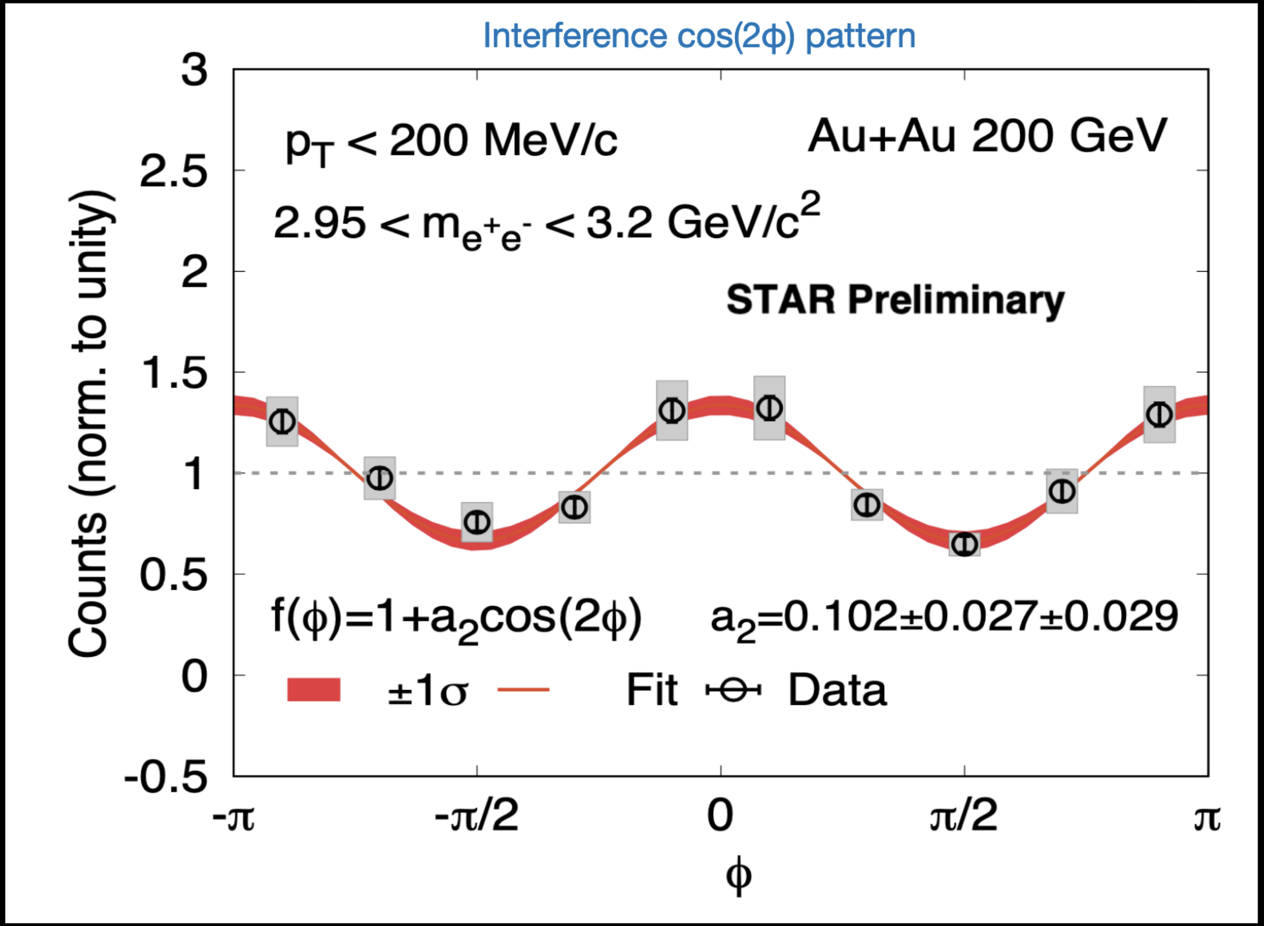

Observed spin interference for J/ψ → e^+e^-

Corrections of interference signal due to 2γ background

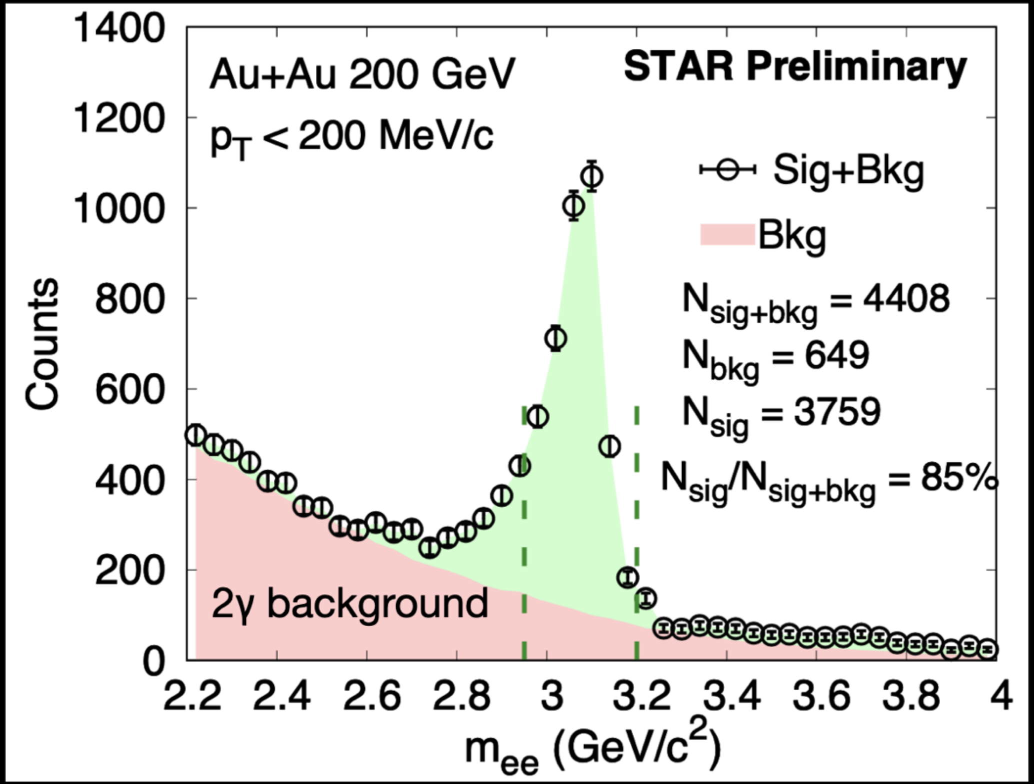

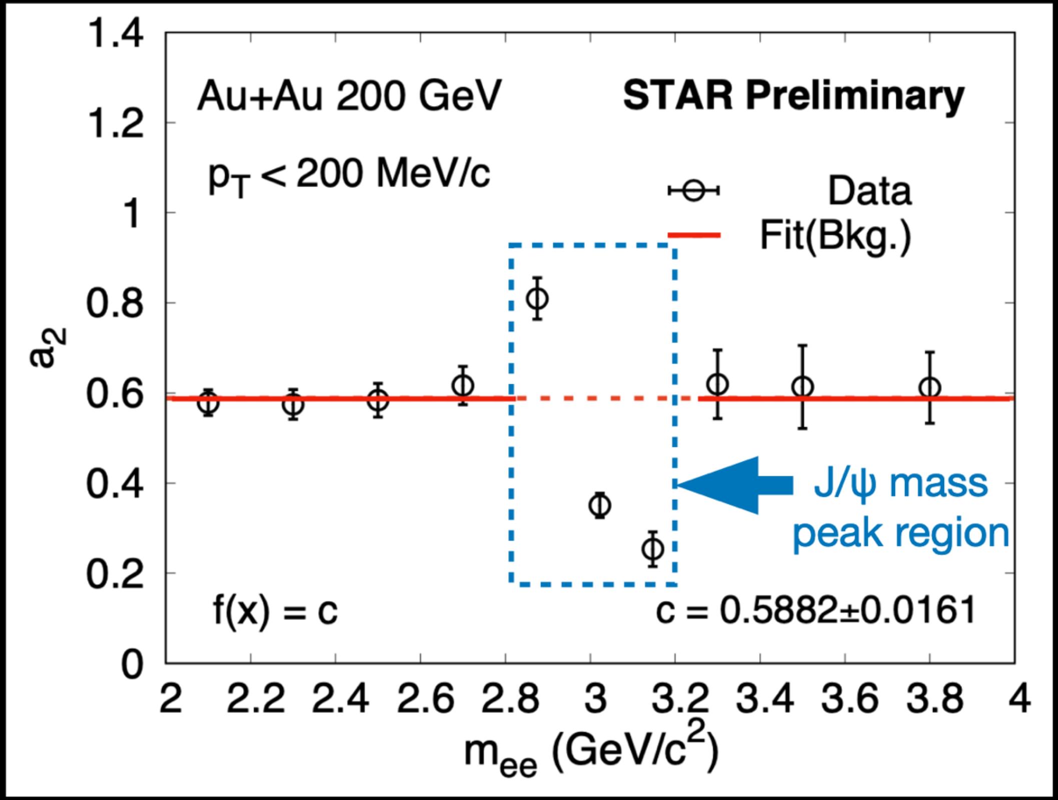

- The $\gamma + \gamma \rightarrow e^+ + e^-$ has also the J/Ψ interference like pattern due to detector effect
- We correct for the 2γ process with : $a_2 = f \times a_2^{bkg} + (1-f) \times a_2^{sig}$, with $f = \frac{N_{bkg}}{N_{sig} + N_{bkg}}$

=> Background correction is done to extract true modulation signal

Corrections of interference signal due to bremsstrahlung process

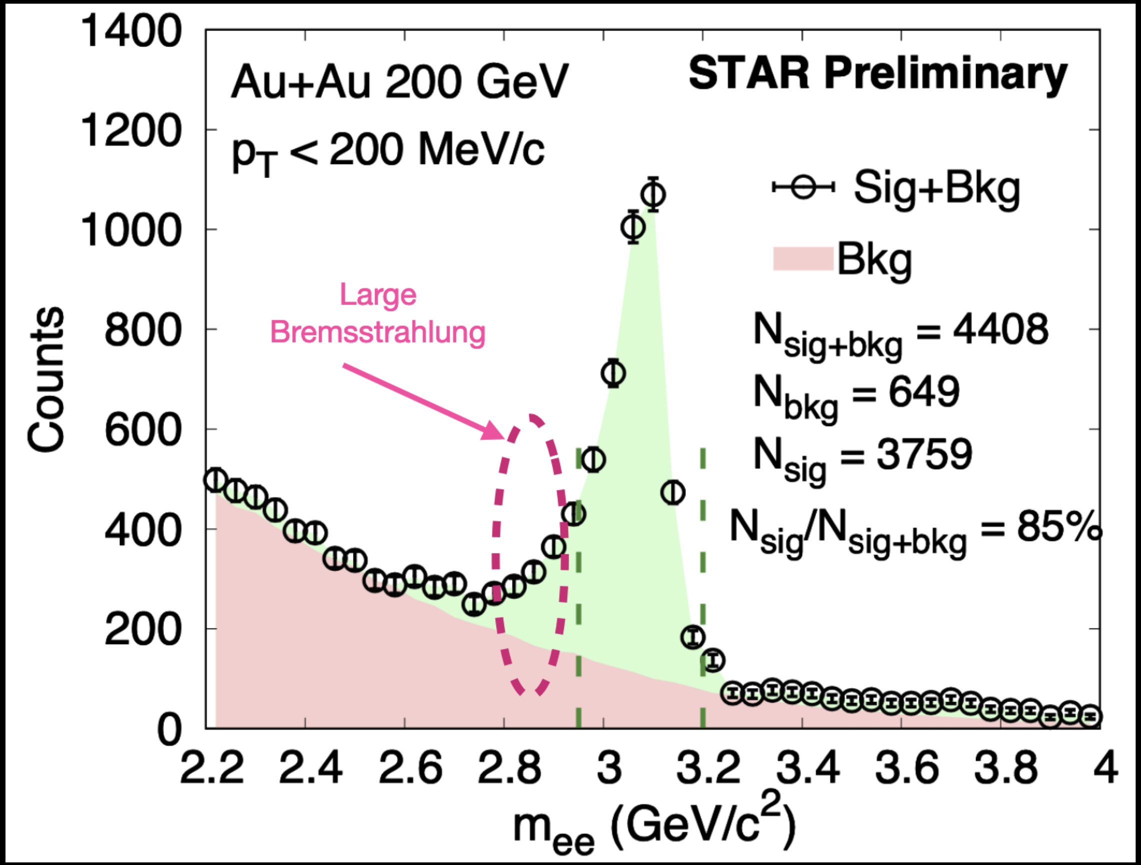

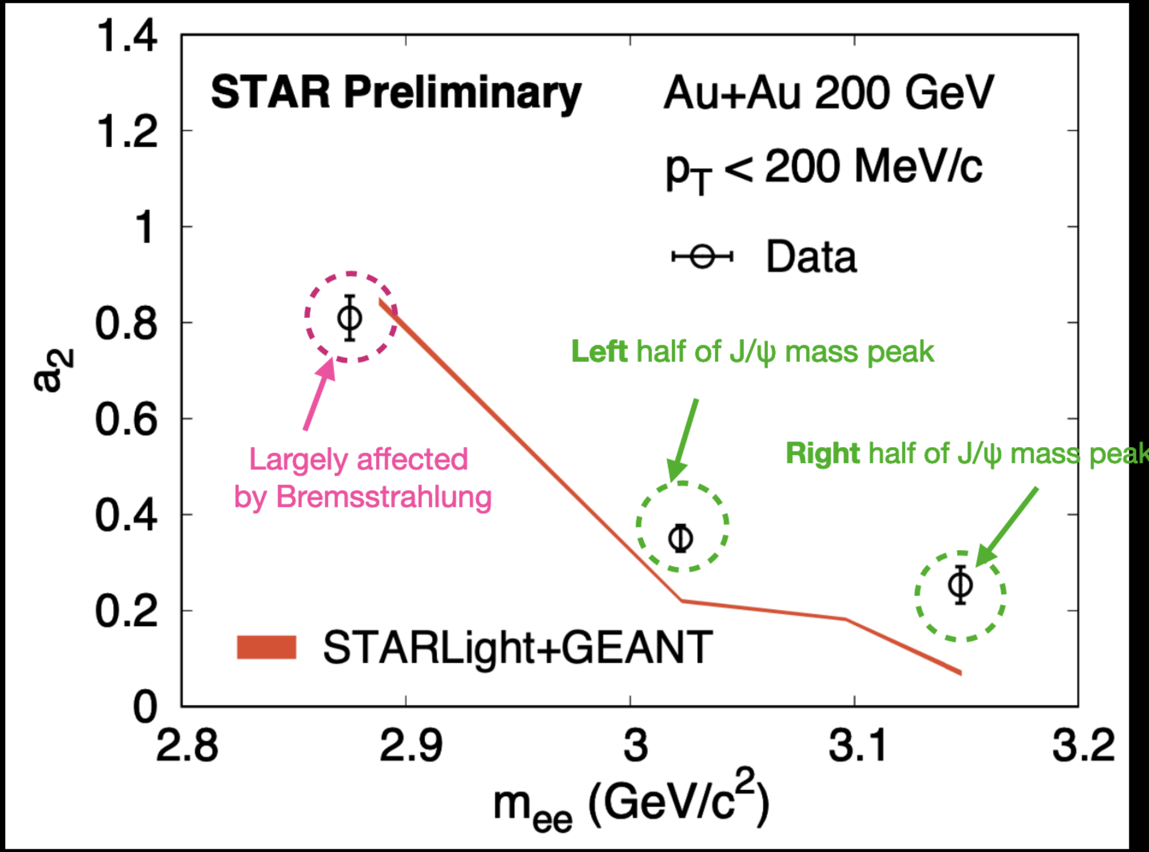

- We considered the Bremsstrahlung process and $J/\Psi \rightarrow e^+ + e^- + \gamma$, using the STARLight+Geant simulations

=> Bremsstrahlung correction performed for true modulation signal

Signal for J/ψ Spin interference

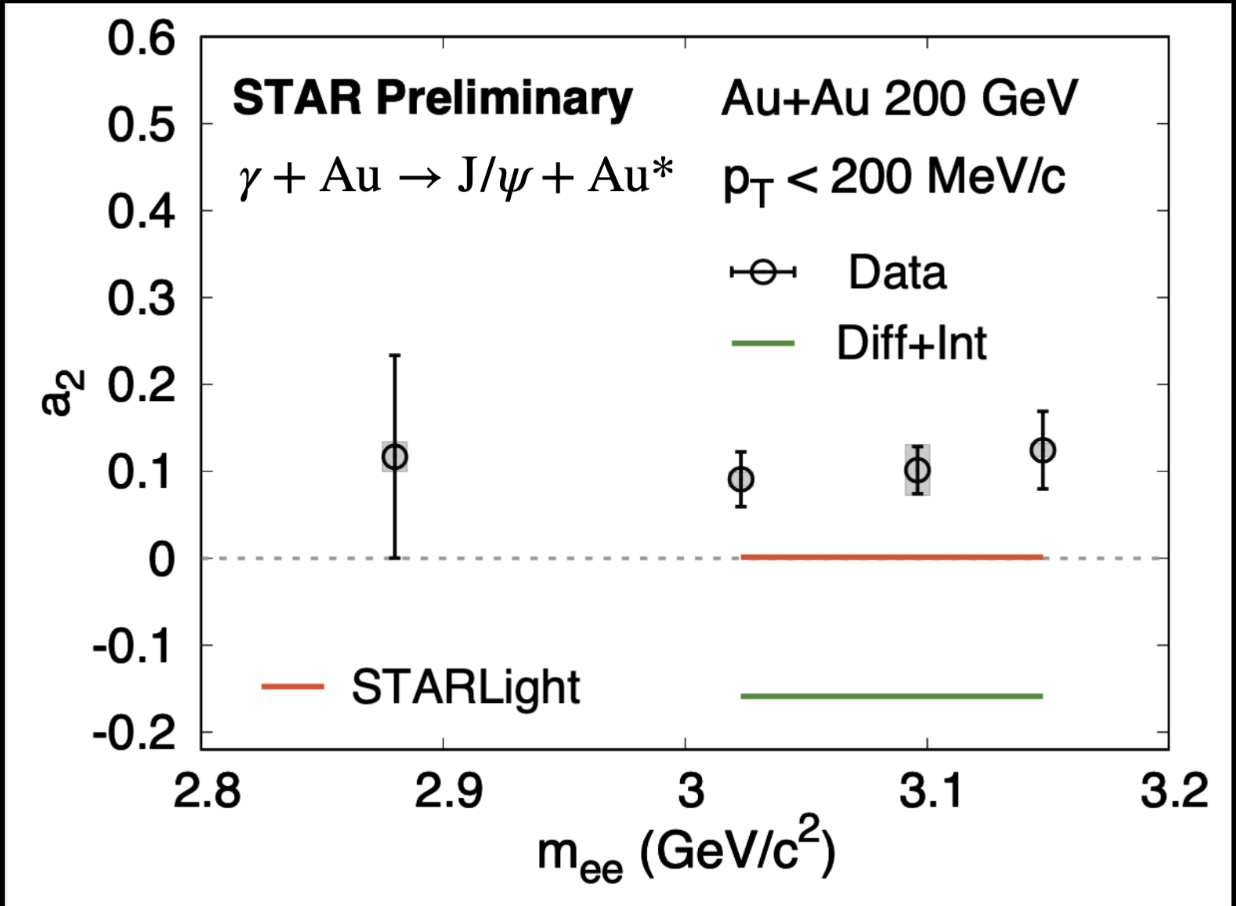

- Measured and corrected signal for J/Ψ spin interference:

$$a_2 = 0.102 \pm 0.027 \pm 0.029$$

- Measurement has ~3σ significance above zero
- Compared with STARLight and theory calculations
- STARLight has no spin interference physics — consistent with zero
- Theory (Diffractive+Interference) predicts negative modulation

Diff+Int predictions : Mäntysaari et al. Phys.Rev.C 109 (2024) 2, 024908

=> Observed spin interference signal ~10% in the measured kinematic range

The p_T-dependent interference of J/ψ

- Interference signal shows strong p_T dependence and rises toward positive
- STARLight predicts zero
- Diffractive+interference calculations are negative at low and high p_T
- Diffractive+interference with additional soft γ radiation predicts negative at low p_T and rises towards positive value at higher p_T

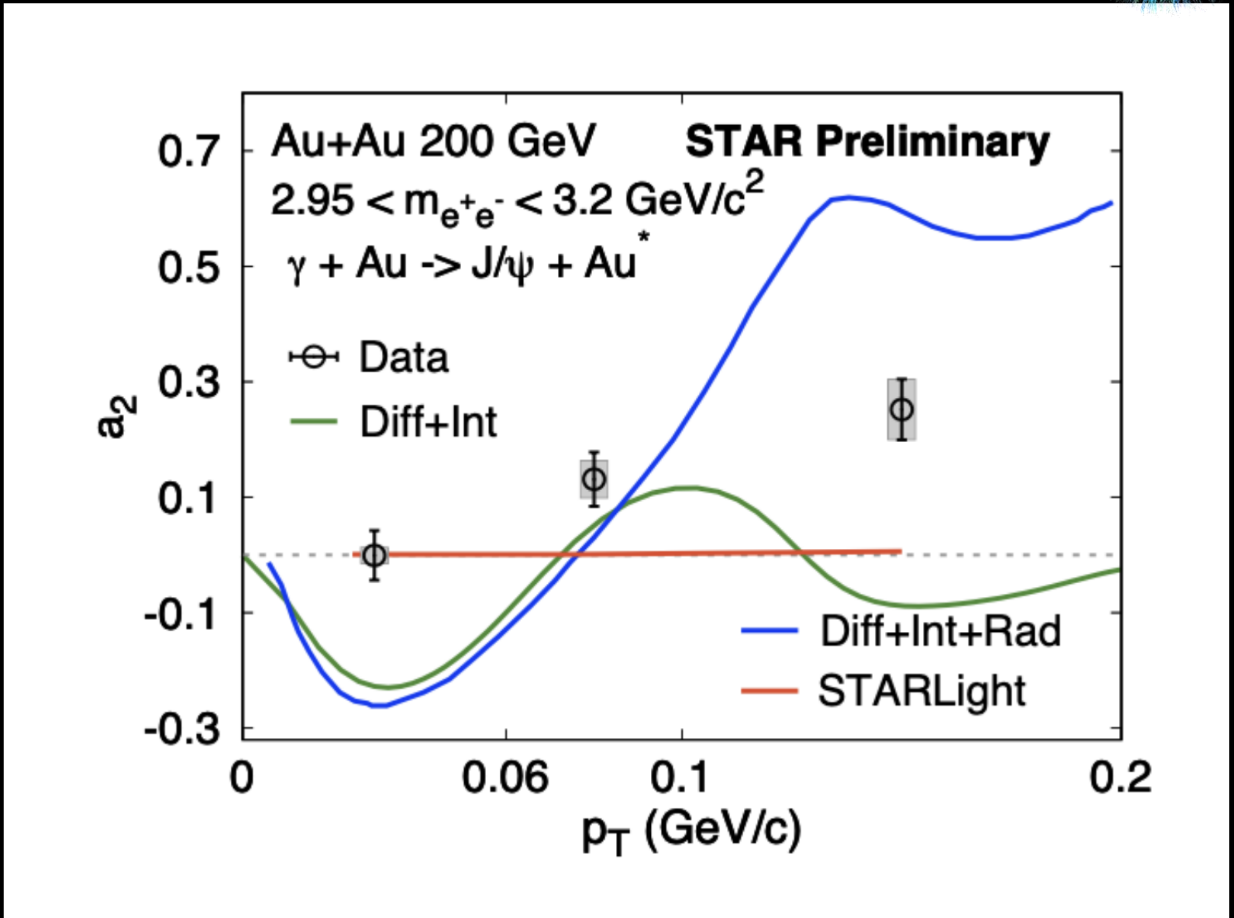

Diff+Int predictions : Mäntysaari et al. Phys.Rev.C 109 (2024) 2, 024908
Diff+Int+Rad predictions : Brandenburg et. al, Phys. Rev. D 106, 074008 (2022)

=> Modulation strength in data positively increases with p_T in the measured kinematics

Baryon number carrier and its transport

What carries the baryon number?

https://en.wikipedia.org/wiki/Proton
https://en.wikipedia.org/wiki/Baryon

In particle physics, the **baryon number** is a strictly conserved additive quantum number of a system.

Baryons, along with mesons, are hadrons, particles composed of quarks. Quarks have baryon numbers of $B = \frac{1}{3}$ and antiquarks have baryon numbers of $B = -\frac{1}{3}$. The term "baryon" usually refers to *triquarks*—baryons made of three quarks ($B = \frac{1}{3} + \frac{1}{3} + \frac{1}{3} = 1$).

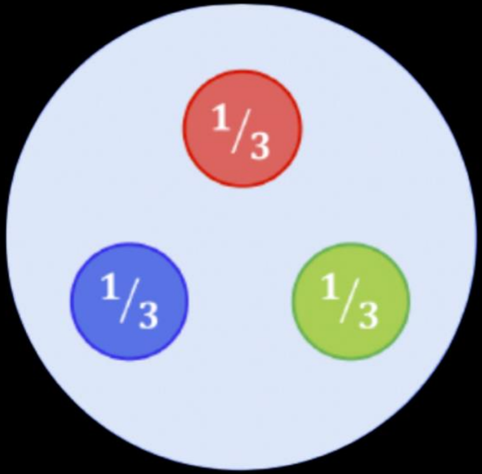

1963-70

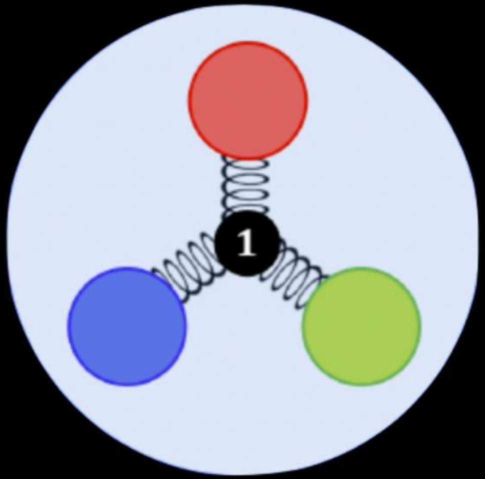

1975-

In conventional picture, baryon number is assumed to be carried by the valence quarks each carrying 1/3

Goldberg and Y. Ne'eman, Nuovo Cimento 27 (1963) 1
Gell-Mann, Zweig, 1964, SLAC 1970
Review: hep-ph/9301246

Baryon number may flow with the flow of the Y-shaped string junction (QCD topology)

X. Artru, Nucl. Phys. B 85, 442–460 (1975), G.C. Rossi and G. Veneziano, Nucl. Phys.B123(1977) 507; Phys. Rep.63(1980) 149
Kharzeev, Phys. Lett. B, 378 (1996) 238-246

No experiment has conclusively established the true carrier of baryon number, two different carriers for Q & B inside a baryon possible

Gluonic junction as a carrier of baryon number

Kharzeev, Phys. Lett. B, 378 (1996) 238-246, Lewis et. al, arXiv:2205.05685

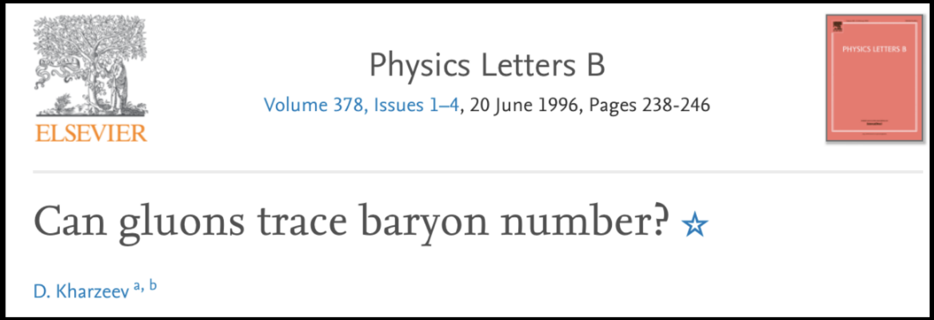
Physics Letters B

Volume 378, Issues 1–4, 20 June 1996, Pages 238-246

Can gluons trace baryon number? ☆

D. Kharzeev[a, b]

Junction-Junction

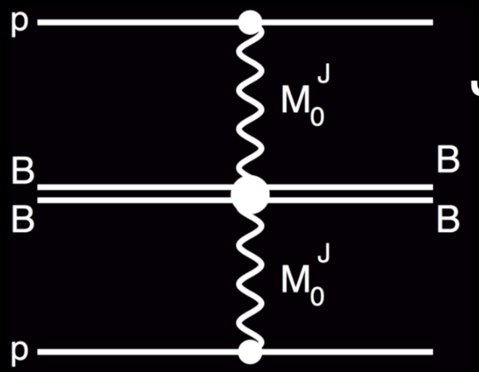

Junction-Pomeron

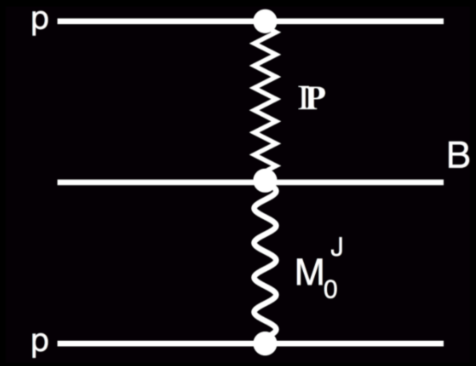

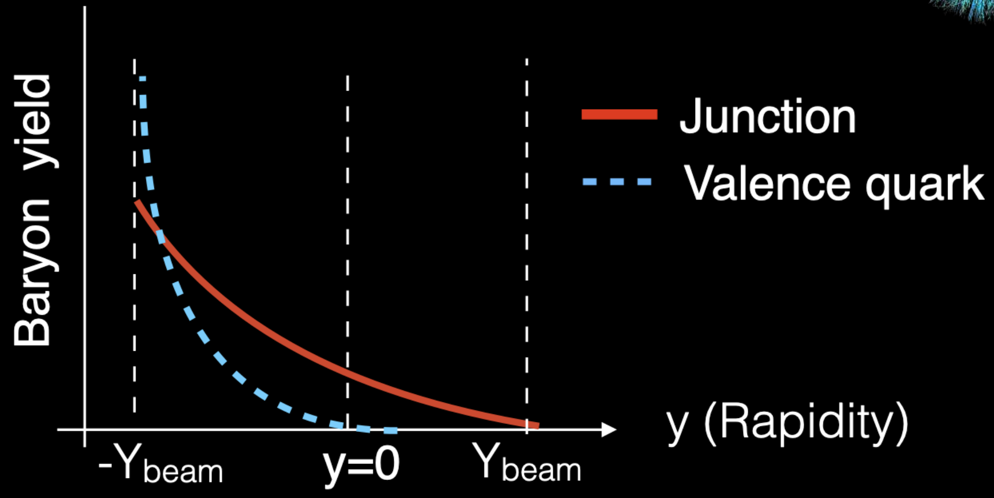

Baryon junction: $e^{-\alpha_B(y-Y_{\mathrm{beam}})}$ $0.42 \leq \alpha_B \leq 1$

PYTHIA 6 (Quarks): $e^{-2.5(y-Y_{\mathrm{beam}})}$

Regge theory can predict rapidity dependence of baryon stopping for junctions

Larger transport to mid-rapidity for gluonic junction than valence quarks as baryon carrier

Strategies for tracing the baryon carrier

Check if charge and baryon are carried by the same object

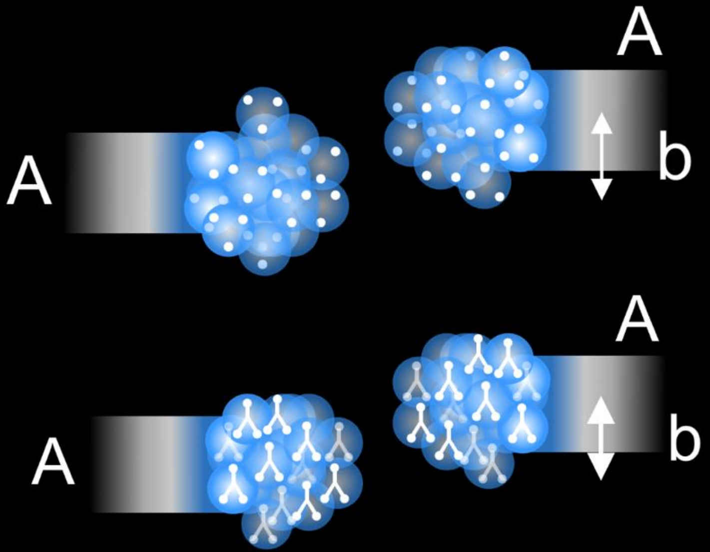

Compare electric-charge with baryon transport

Q <-> Z/A x B

Test expectations for valence quark transport with rapidity & centrality

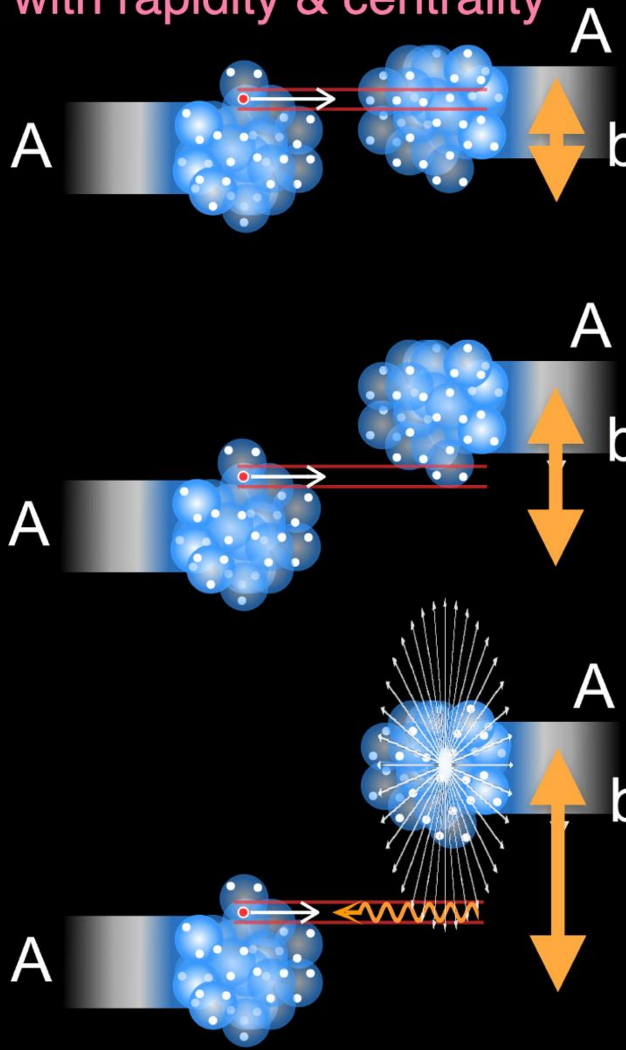

Centrality dependence of dN/dy(B) vs. $y\text{-}Y_{beam}$

Test if the baryon carrier is a gluonic object by colliding with a photon of very small stopping power

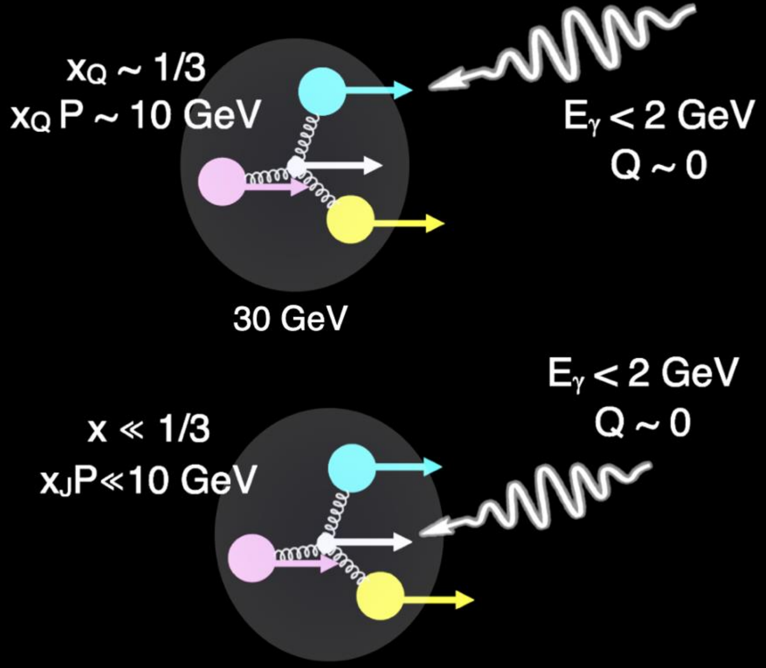

Rapidity dependence of dN/dy(B) in γ+A collisions

Electric charge vs. baryon transport

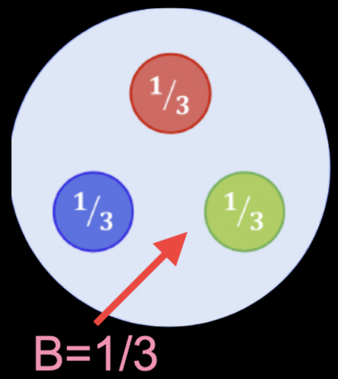

Valence quarks carry electric charge & baryon

$$\text{Charge stopping} \simeq \frac{Z}{A} \times \text{Baryon stopping}$$

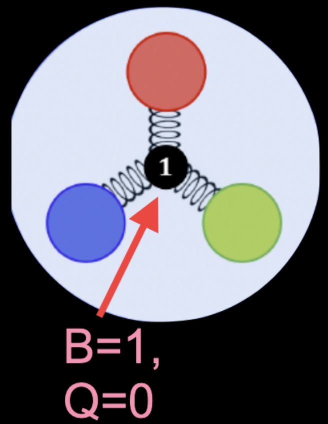

Valence quarks carry electric charge & junction carry baryon

$$\text{Charge stopping} < \frac{Z}{A} \times \text{Baryon stopping}$$

Baryon transport at mid-rapidity:

$$B = (N_p - N_{\bar{p}}) + (N_n - N_{\bar{n}})$$

Not difficult except for "n" measurement

Charge transport at mid-rapidity:

$$Q = (N_{\pi^+} + N_{K^+} + N_p) - (N_{\pi^-} + N_{K^-} + N_{\bar{p}})$$

Precision measurement is difficult : isospin conservation, efficiency effects

ΔQ and B transport should correlated for valence quark picture not for junctions

Precision measurements in isobar collisions

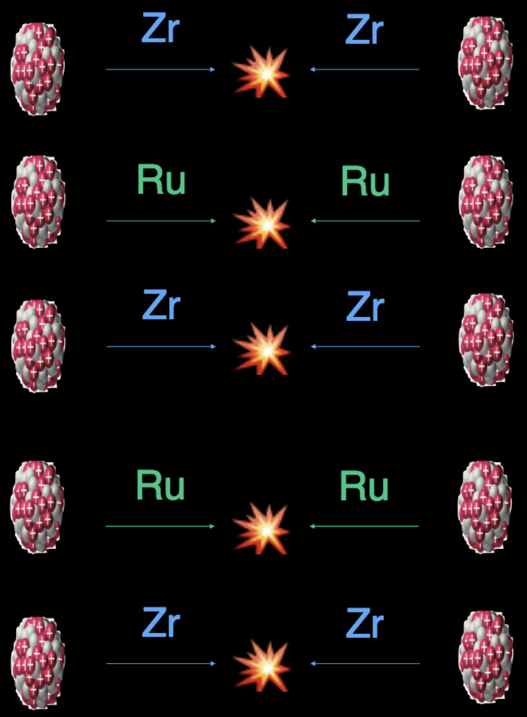

Zirconium:
A=96 (Total baryon)
Z=40 (Total charge)

Ruthenium:
A=96 (Total baryon)
Z=44 (Total charge)

Overcome precision problem: 1) compare two isobars, 2) express difference as ratios:

$$R2_\pi = \frac{(N_{\pi^+}/N_{\pi^-})^{\mathrm{Ru}}}{(N_{\pi^+}/N_{\pi^-})^{\mathrm{Zr}}}$$

Q transport difference between isobars:

$$\Delta Q = N_\pi \left[(R2_\pi - 1) + \frac{N_K}{N_\pi}(R2_K - 1) + \frac{N_p}{N_\pi}(R2_p - 1) \right]$$

Neutron using deuteron, proton

B transport, same in two isobars:

$$B = (N_p - N_{\bar{p}}) + (N_n - N_{\bar{n}})$$

$$\frac{N_{\bar{n}}}{N_n} = \frac{N_p}{N_{\bar{p}}} \frac{N_{\bar{d}}}{N_d}$$

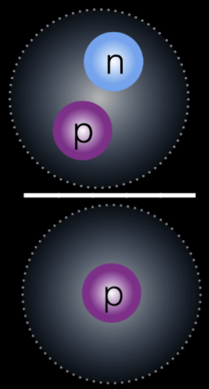

Using isobar goal is to test: $\Delta Q \leftrightarrow \frac{\Delta Z}{A} \times B$

Precision measurements in isobar collisions

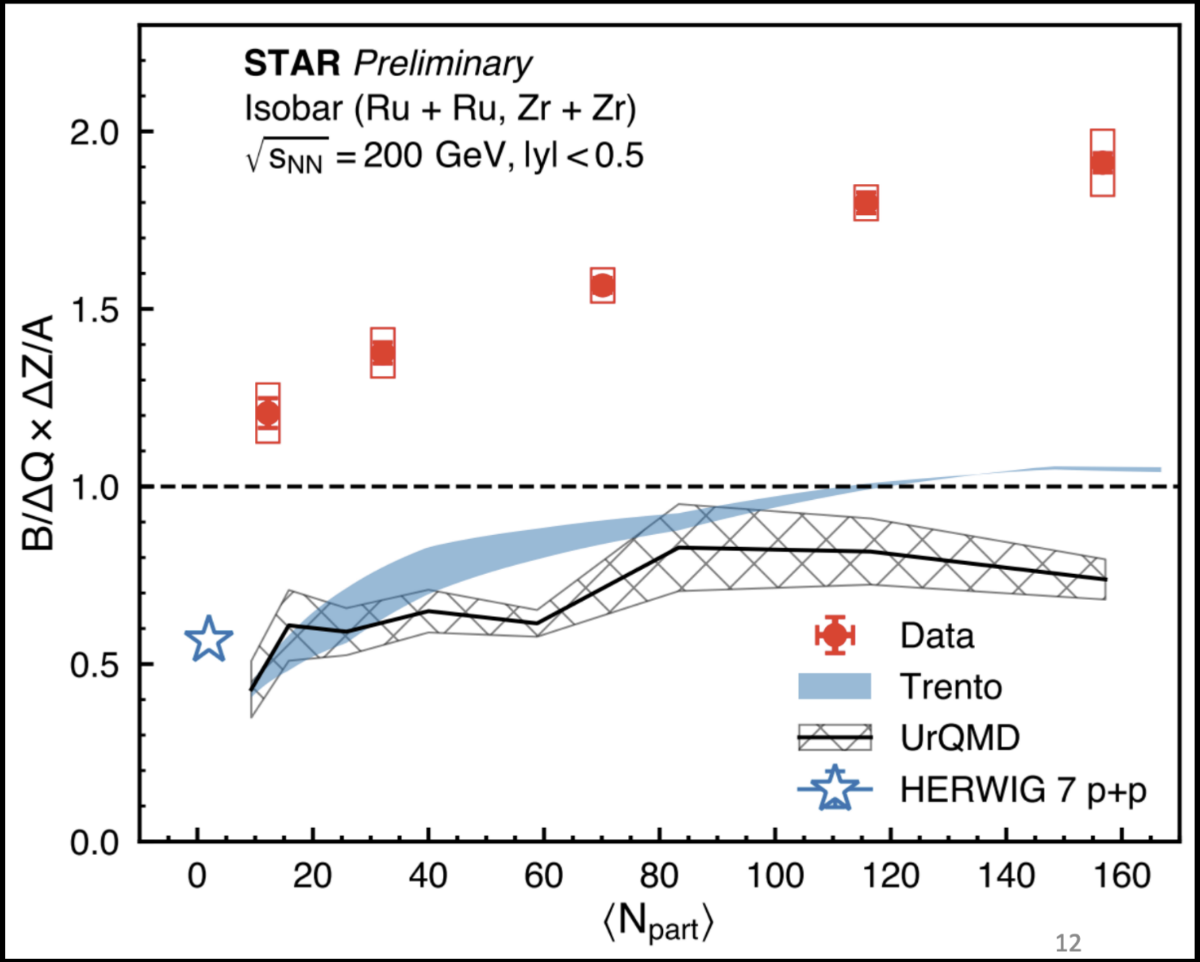

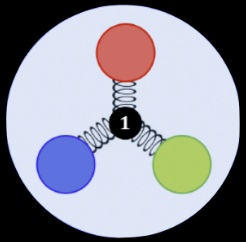

First measurements of electric charge stopping using isobar collisions

Data: More baryon transported to central rapidity than electric charge

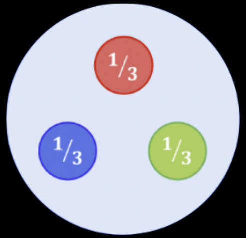

Non-junction models (UrQMD, HERWIG): equal or less baryon compared to electric charge

Not compatible with same carrier of electric charge and baryon

Rapidity distribution of baryon production: Global data

STAR data: N. Lewis, et. al., arXiv:2205.05685, BRAHMS+NA49: F. Videbaek, 1st workshop on baryon dynamics, SBU, 2024

Baryon transport with rapidity loss ($y-Y_{beam}$)

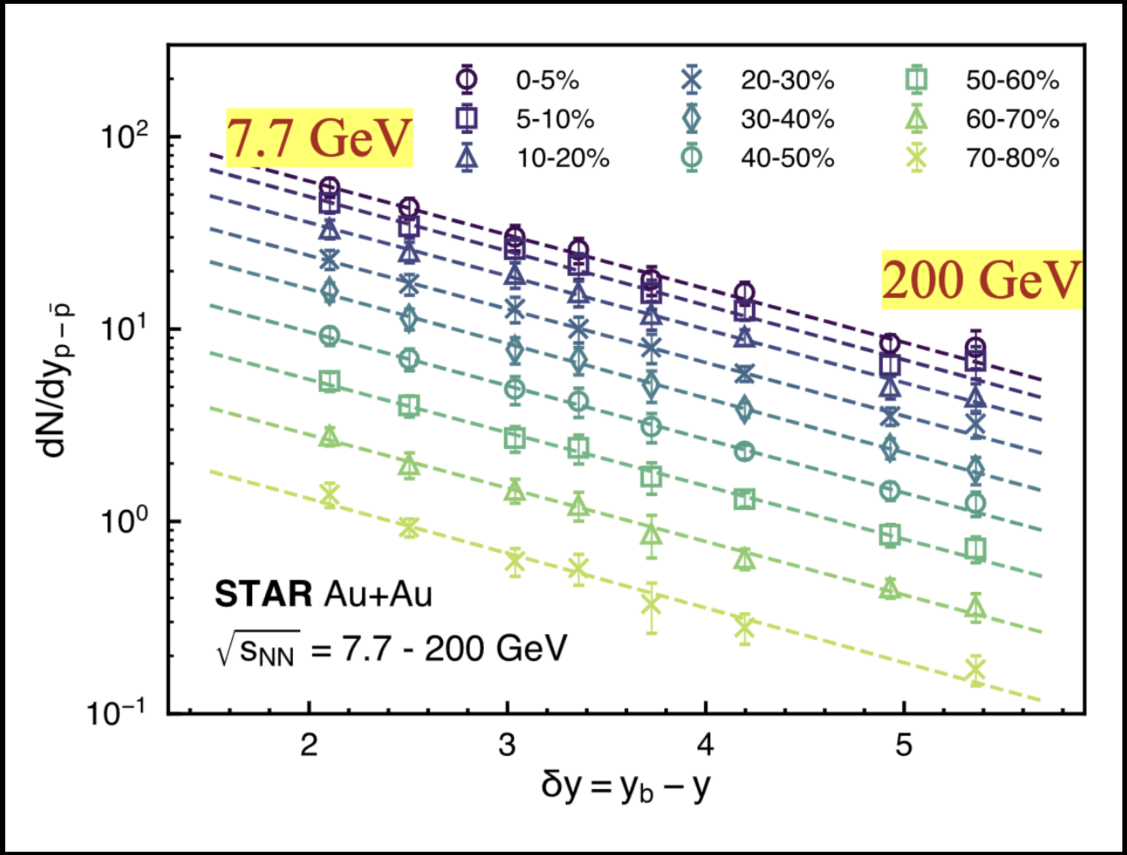

Exponential with slope 0.63±0.2, no change with centrality for $2<Y_{beam}<5.5$

BRAHMS + NA49 data (wider $y-Y_{beam}$)

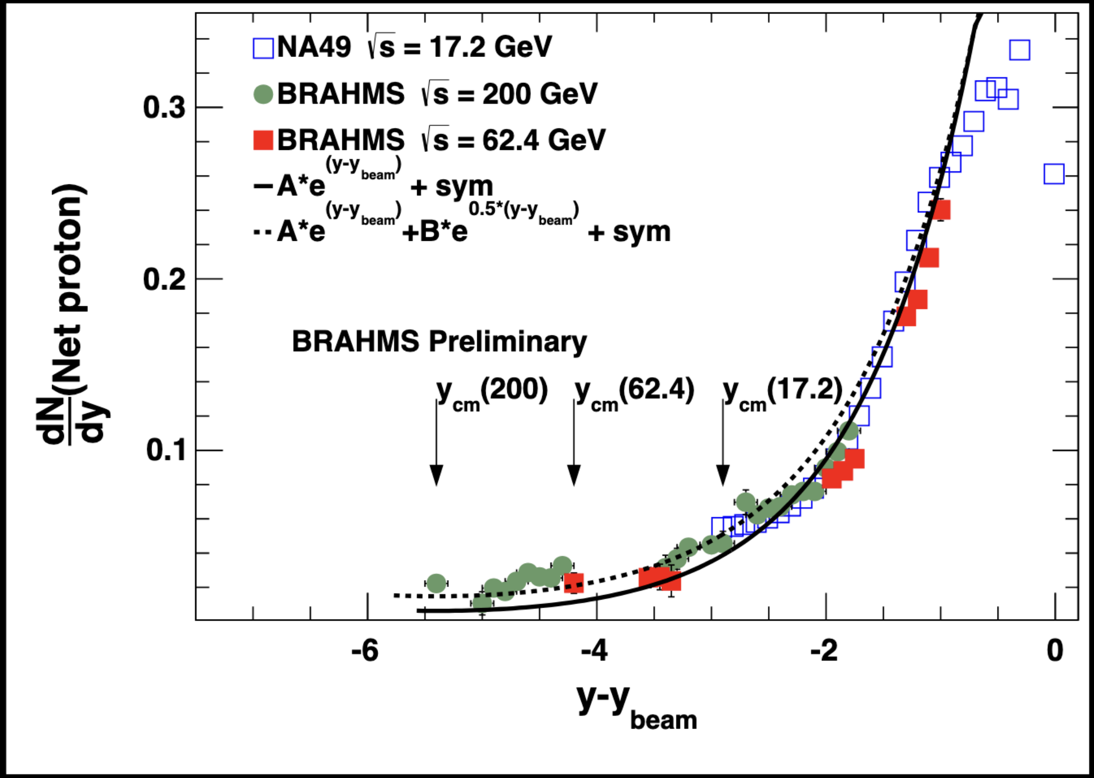

At higher energy rapidity slope closer to~0.5 lower energy ($|y-Y_{beam}|<2$) rapidity slope ~1

Rapidity slope of baryon density: centrality independent, depends on $|y-Y_{beam}|$ range

Probing baryon structure with photon-induced processes

Fig: Lewis et. al, arXiv: 2205.05685, Sweger, CA EIC consortia meet

We trigger on γ+Au events in Ultra-peripheral collisions of Au+Au at 54.4 GeV
Approximate γ+Au $\sqrt{s_{\gamma N}}$~10 GeV

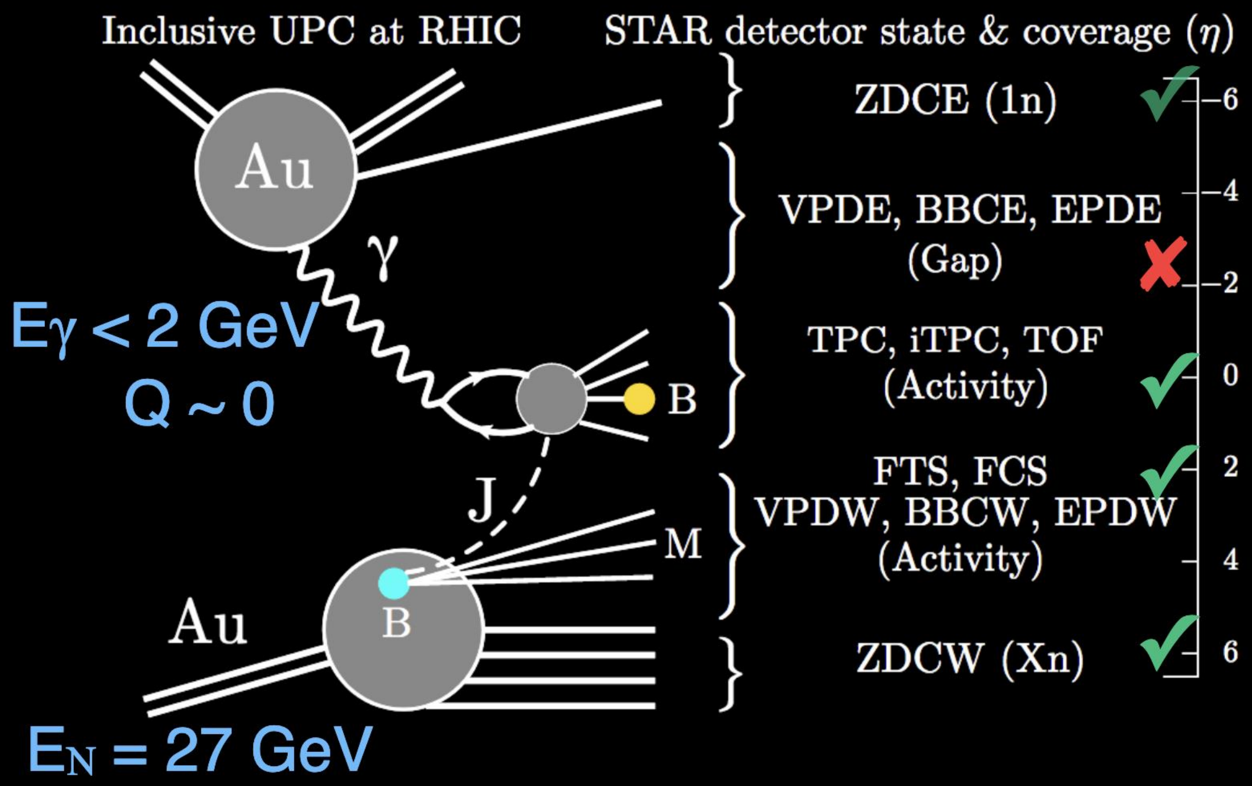

UPC photons have very low stopping power

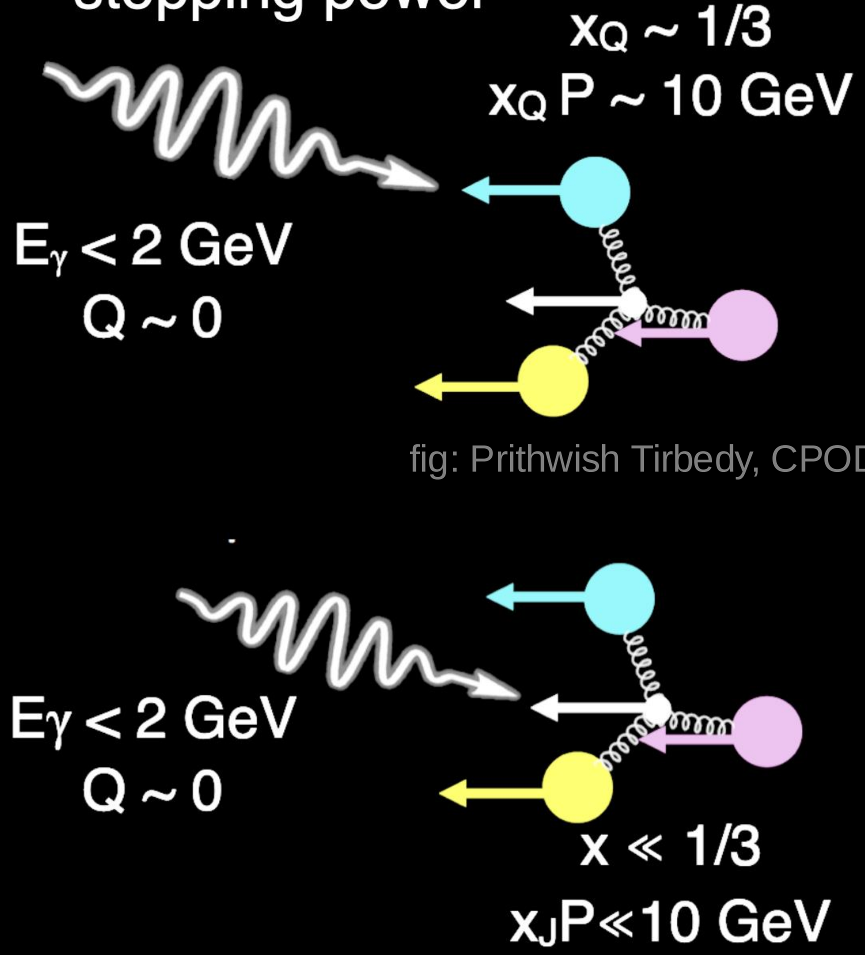

fig: Prithwish Tirbedy, CPOD 2024

Search for non-zero net-baryon in photon-ion collisions near central-rapidity

Triggering inclusive photon-induced processes by the STAR detector

Lewis et. al, arXiv: 2205.05685, BeAGLE: W. Chang, et al PRD 106, 012007 (2022)

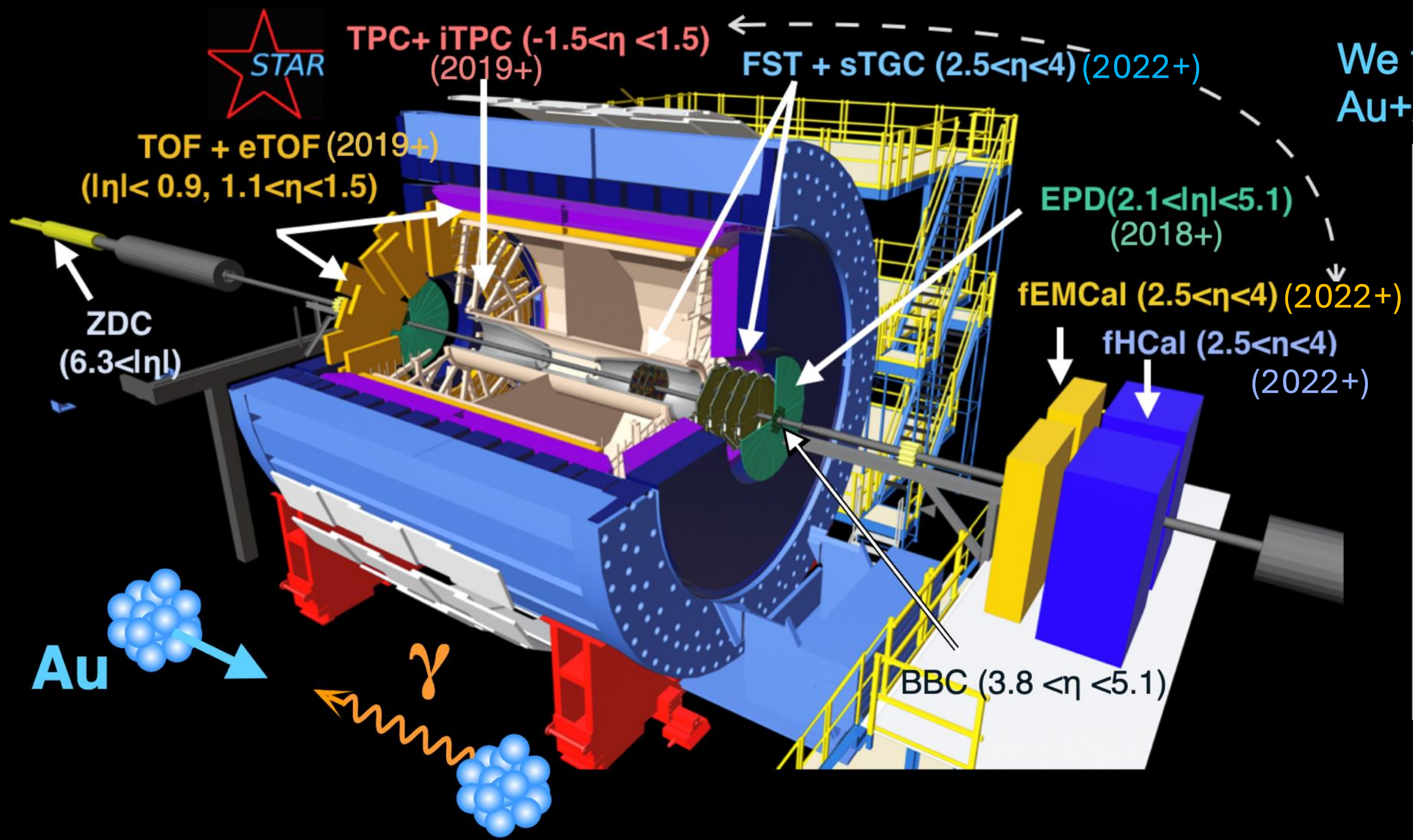

We trigger γ+Au events in ultra-peripheral Au+Au collisions at $\sqrt{s_{NN}}$ = 54.4 GeV

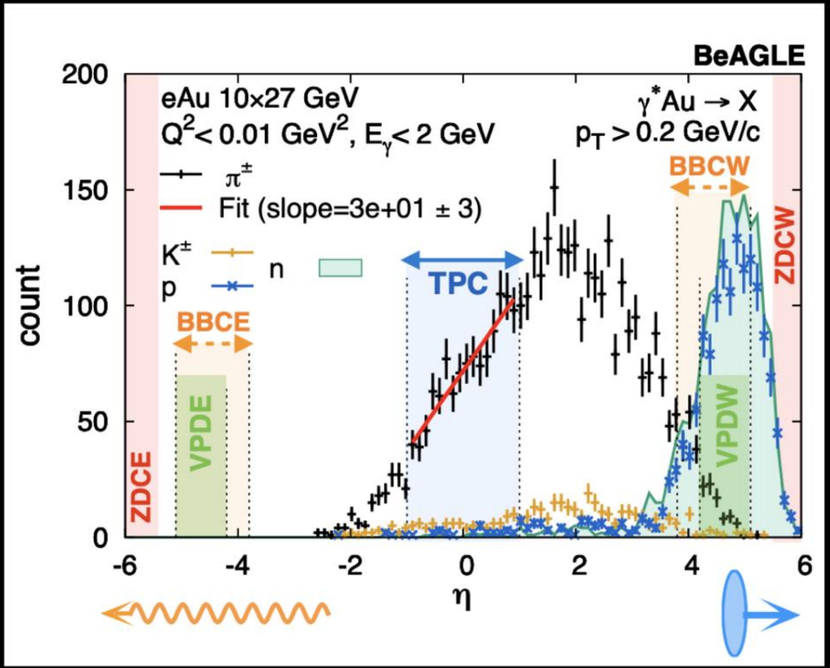

Use characteristic asymmetric particle production to trigger inclusive γ+Au events with help of:

- Beam-Beam counter (BBC),
- Zero-Degree Calorimeter (ZDC),
- Vertex Position Detector (VPD)

Time Projection Chamber (TPC)

- Track reconstruction
- Identify particles using dE/dx

Time-Of-Flight detector (TOF)

- Extend particle identification to high pT
- Pile-up rejection

Results: Rapidity distribution of net-proton in γ+Au events

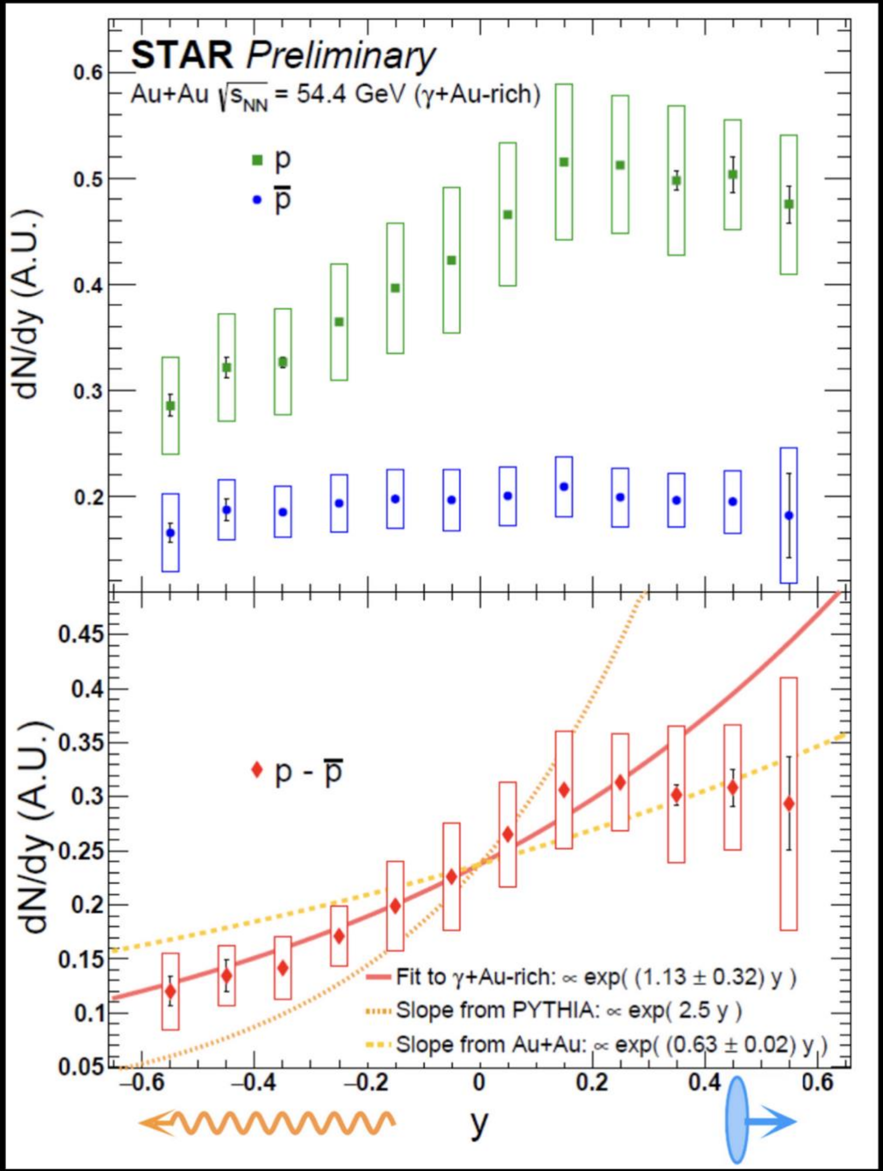

p and net-proton dN/dy with y described by an exponential with slope: 1.13 ± 0.32

Anti-proton distribution is near constant with y

Compared Au+Au slope: 0.63 ± 0.02 ($2<Y_{beam}<5.5$)

Compared to PYTHIA, which does not include a baryon junction mechanism, predicts a slope of 2.5

Exponential slope of rapidity dependence of net-proton lower than PYTHIA predictions

Rapidity slope of net-proton: Global data

X. Artru, M. Mekhfi, Nucl. Phys. A 532 (1991) 351
BRAHMS+NA49: Videbaek, 1st workshop on baryon dynamics, SBU 2024

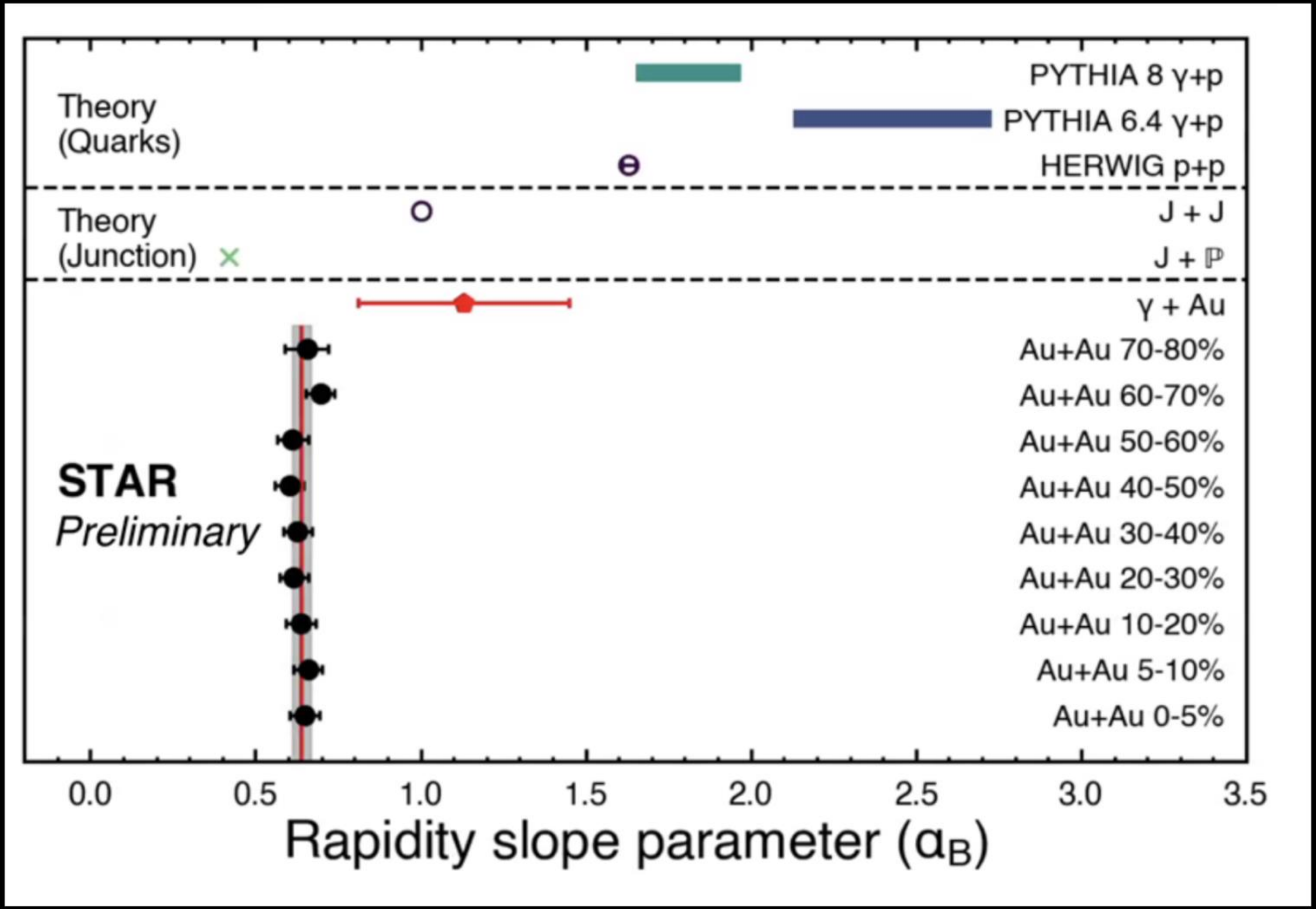

Au+Au slope same for all centrality

Slope γ+Au >~ Slope Au+Au:

Closer to the fit to BRAHMS + NA49 data slope to ~1 for $Y_{beam} < 2$ (NA49 energy ~17 GeV closer to γ+Au cm energy ~ 10 GeV)

Slope has Y_{beam} (energy) dependence

$\alpha_B = \alpha_B(|y - Y_{beam}|)$

Consistent with Regge theory baryon-junction prediction but smaller than PYTHIA/HERWIG

Rapidity dependence of net-proton in γ+Au collisions compatible with junction picture

EM-jet A_N studies at 200 GeV

STAR forward detectors used in the current STAR analyses:

- Forward Meson Spectrometer (FMS): $2.6 < \eta < 4.2$, $\phi \in (0, 2\pi)$; detect γ, π^0, η
- Roman Pot detector (RP): Located about 15 m away from interaction point on both sides; detects slightly scattered protons

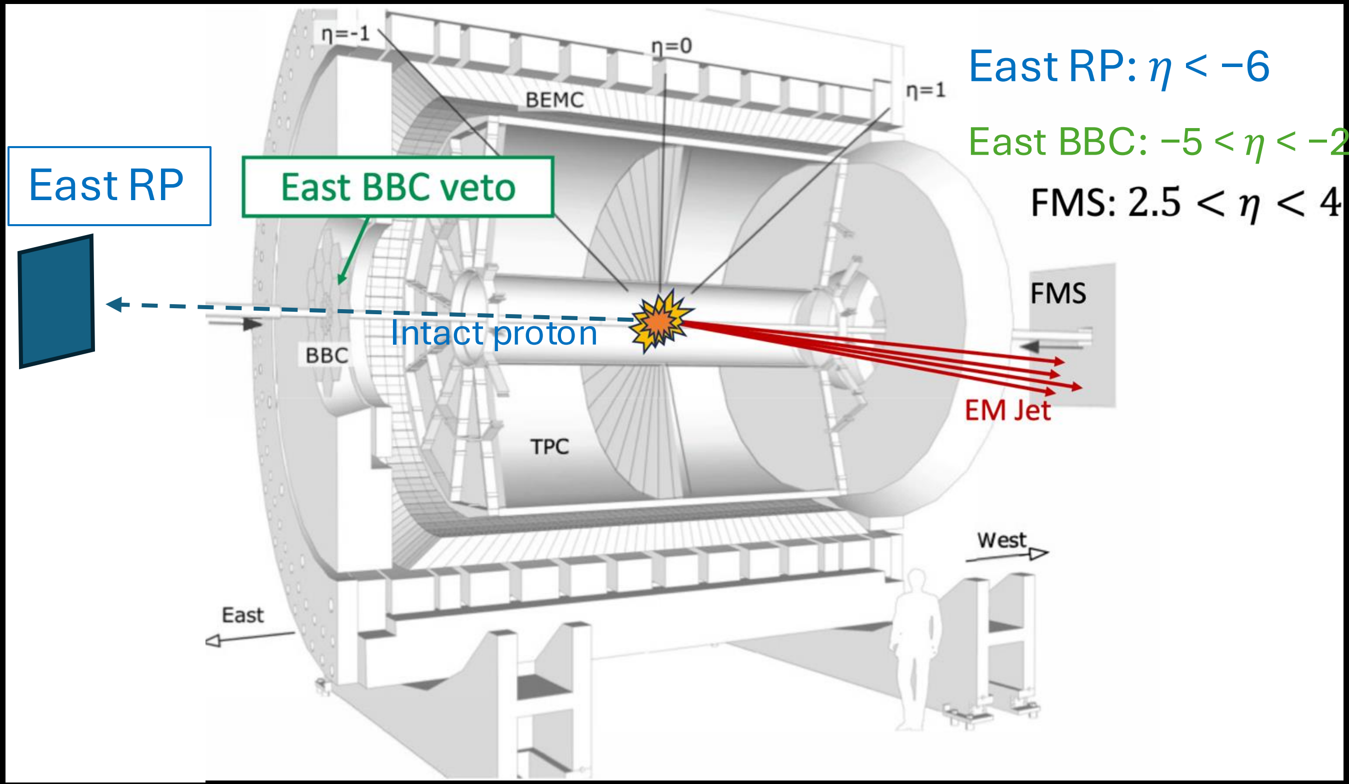

Multi-dimensional studies for inclusive EM-jet A_N at 200 GeV

The ElectroMagnetic jets (EM-jets) are the jets reconstructed using only photons

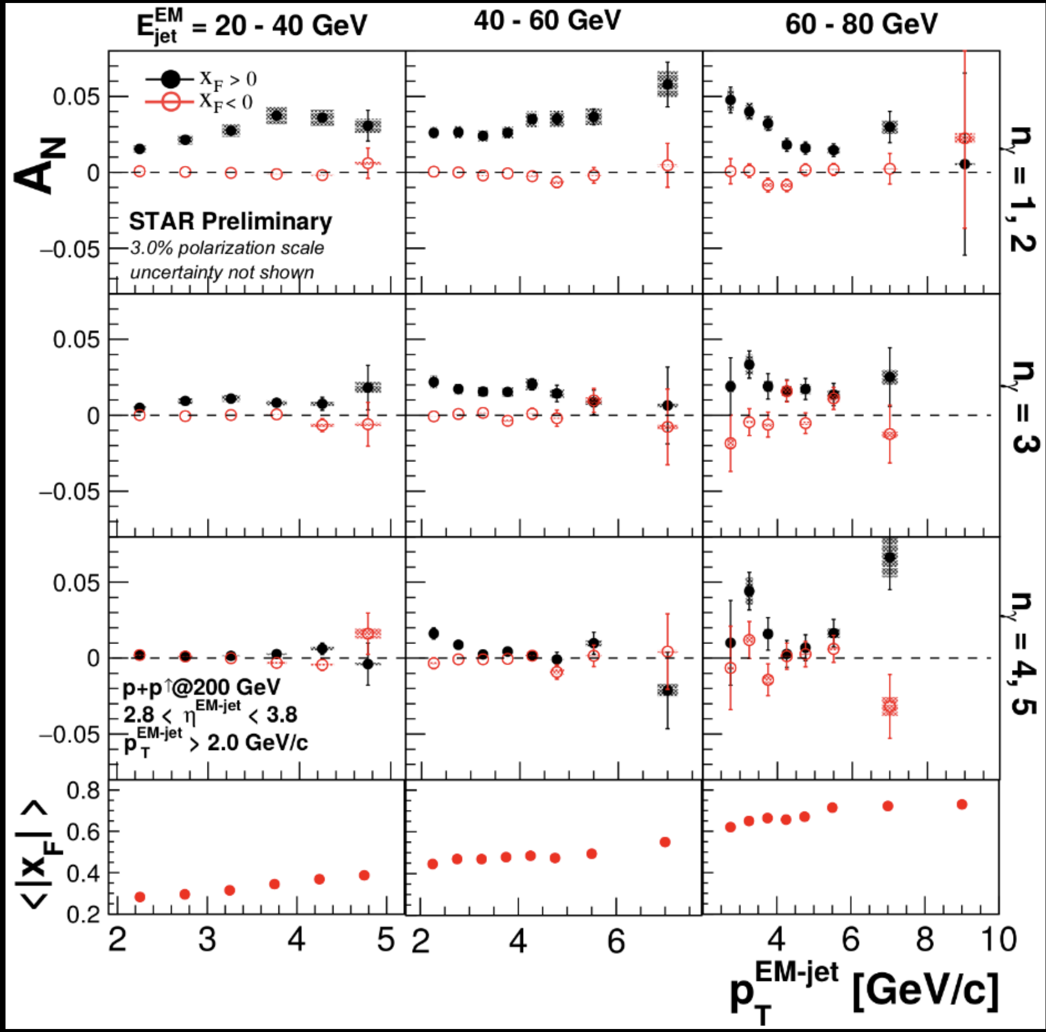

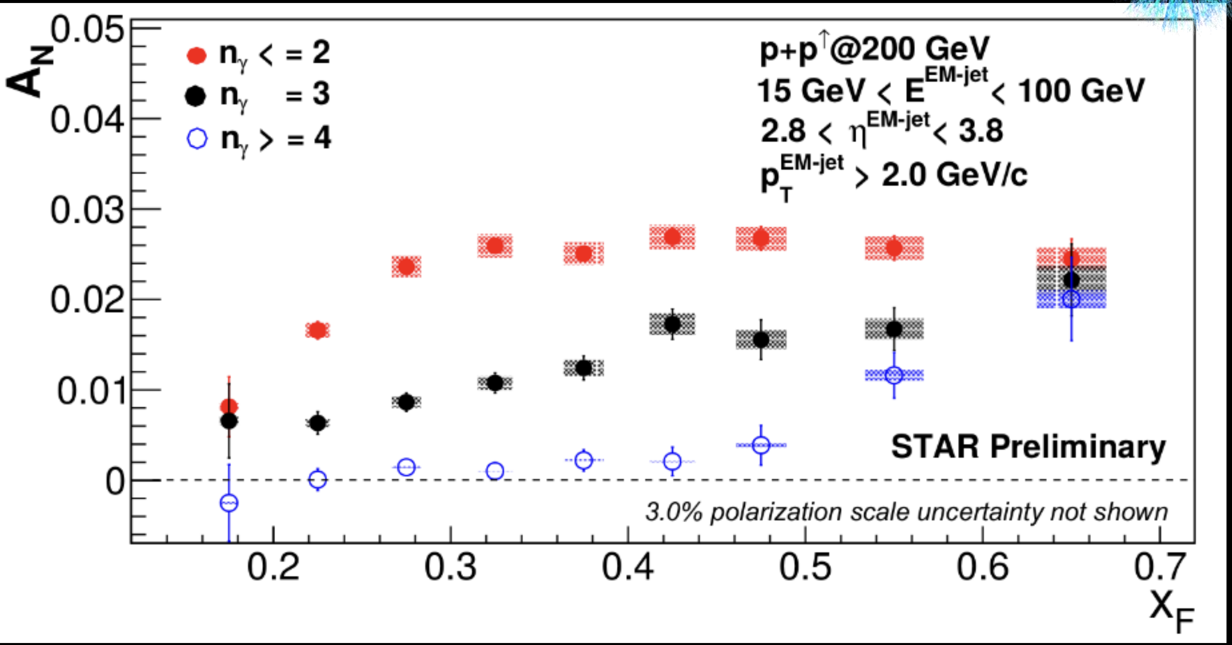

- The EM-jet A_N decreases with increasing photon multiplicity for $x_F > 0$
  - A_N is larger for the EM-jets consisting of 1 or 2 photons
- A_N increases with x_F for all the cases of photon multiplicity

Single diffractive EM-jet A_N at 200 GeV

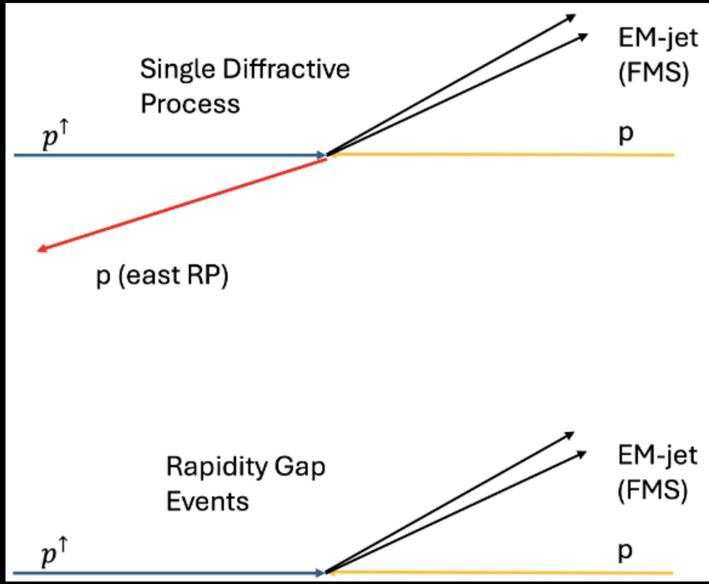

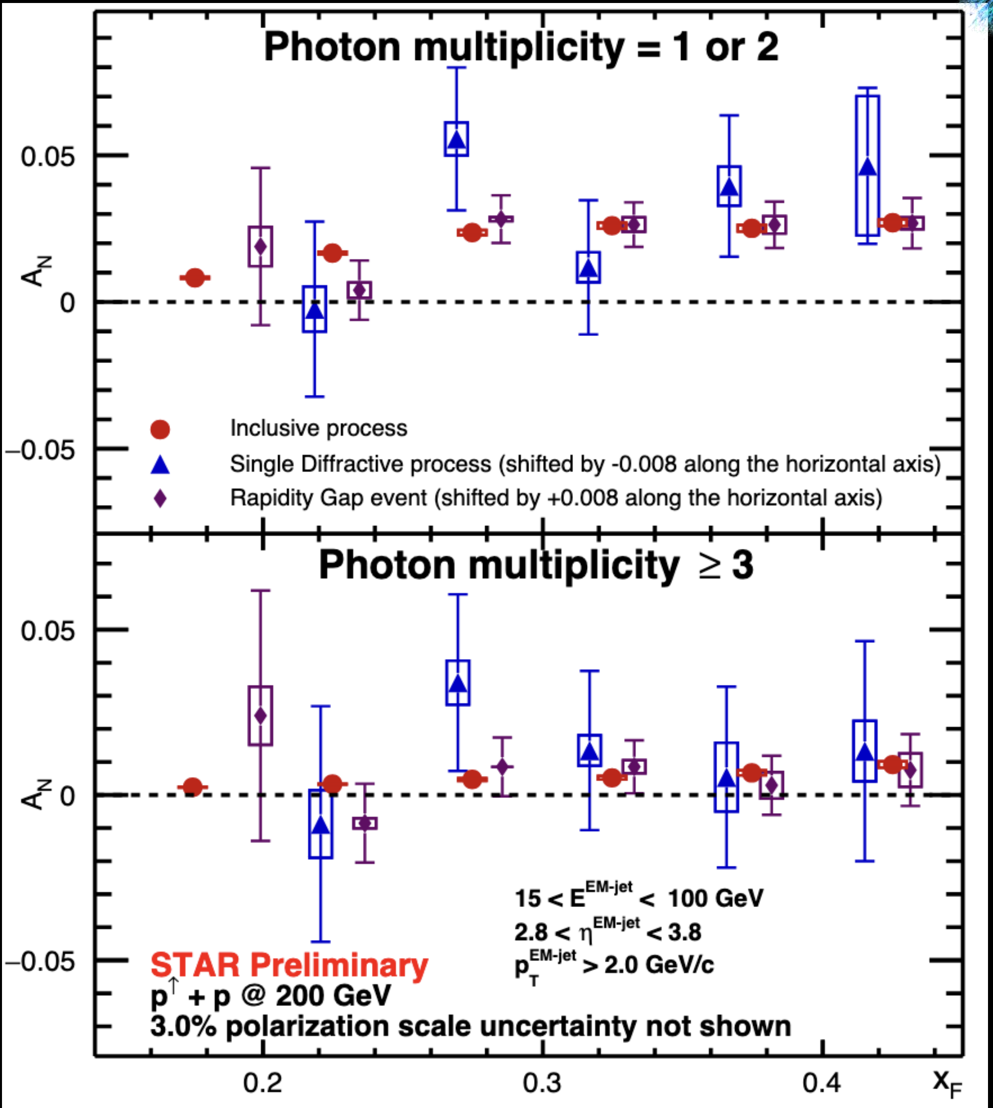

- The EM-jet A_N for $x_F > 0$ (>2σ significance of non-zero) is observed for 1 or 2 photon multiplicity EM-jets in the single diffractive process
- A_N for the three processes consistent with each other within uncertainty
- The single diffractive processes fail to provide evidence for its significant contribution to large A_N in the inclusive processes

Semi-exclusive process EM-jet A_N at 200 GeV

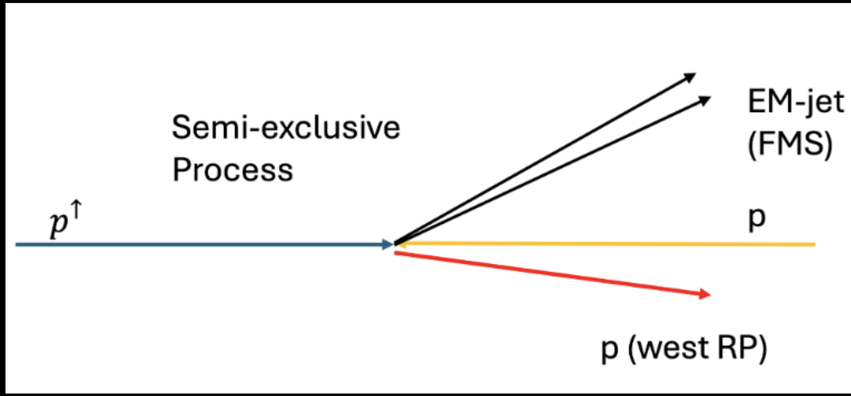

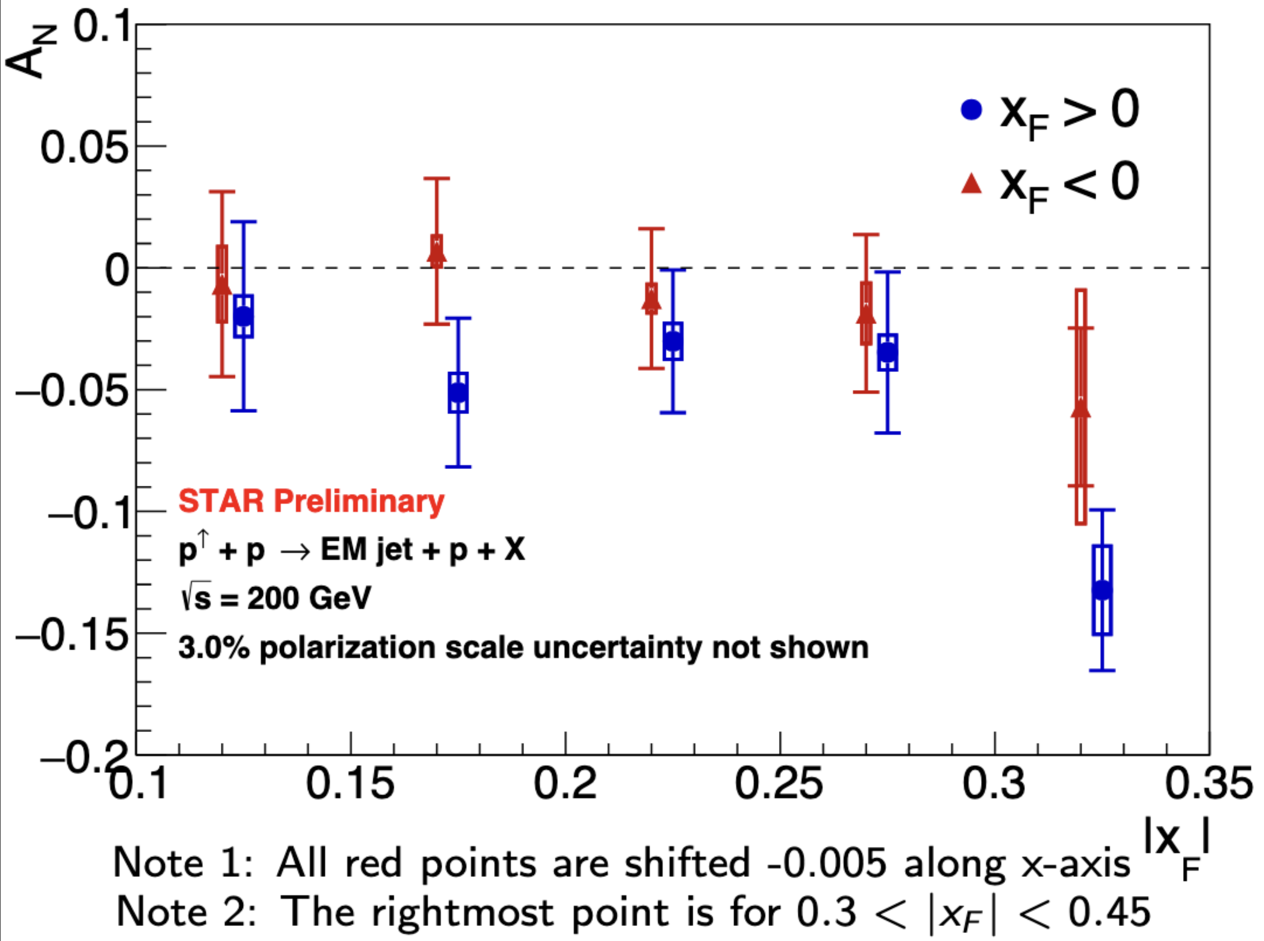

- Semi-exclusive process: polarized proton intact; constrain the energy of EM-jet at FMS and west side proton to less than beam energy
- A non-zero A_N for $x_F > 0$ is observed with 3.3σ significance for the semi-exclusive process
- The sign of A_N is negative. Theoretical inputs are needed to understand the different sign

Nonlinear gluon effects in QCD

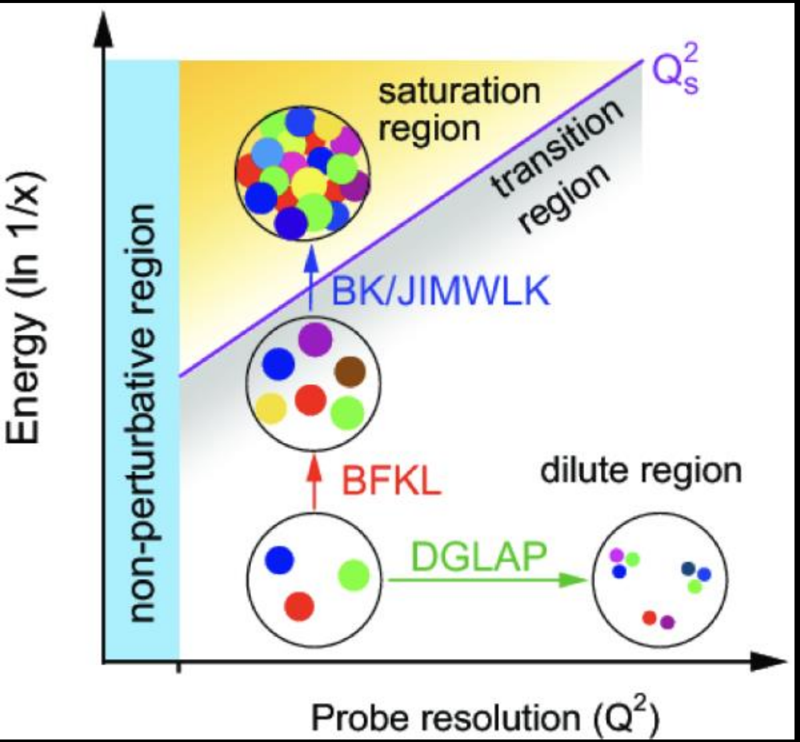

- DGLAP (Dokshitzer Gribov Lipatov Altarelli Parisi): Evolution in resolution Q^2, resums terms in $\alpha_S \log Q^2$ → resolving "smaller" partons at high Q

- BFKL (Balitski Fadin Kuraev Lipatov (BFKL): Evolution in energy x, resums terms in $\alpha_S \log 1/x$ → Large parton densities at small x

- Saturation region at very small x

- Important to understand QCD evolution, parton densities

Nonlinear gluon effects in QCD

M.S. Abdallah et al., Phys. Rev. Lett. 129, 092501

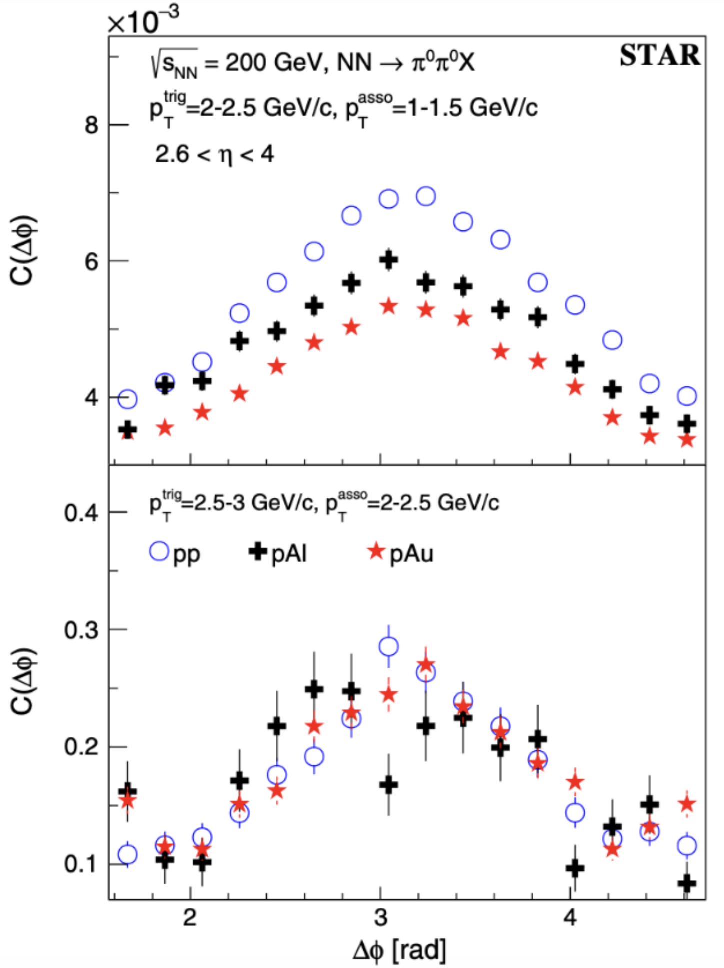

First measurement of the A dependence of nonlinear gluon effects

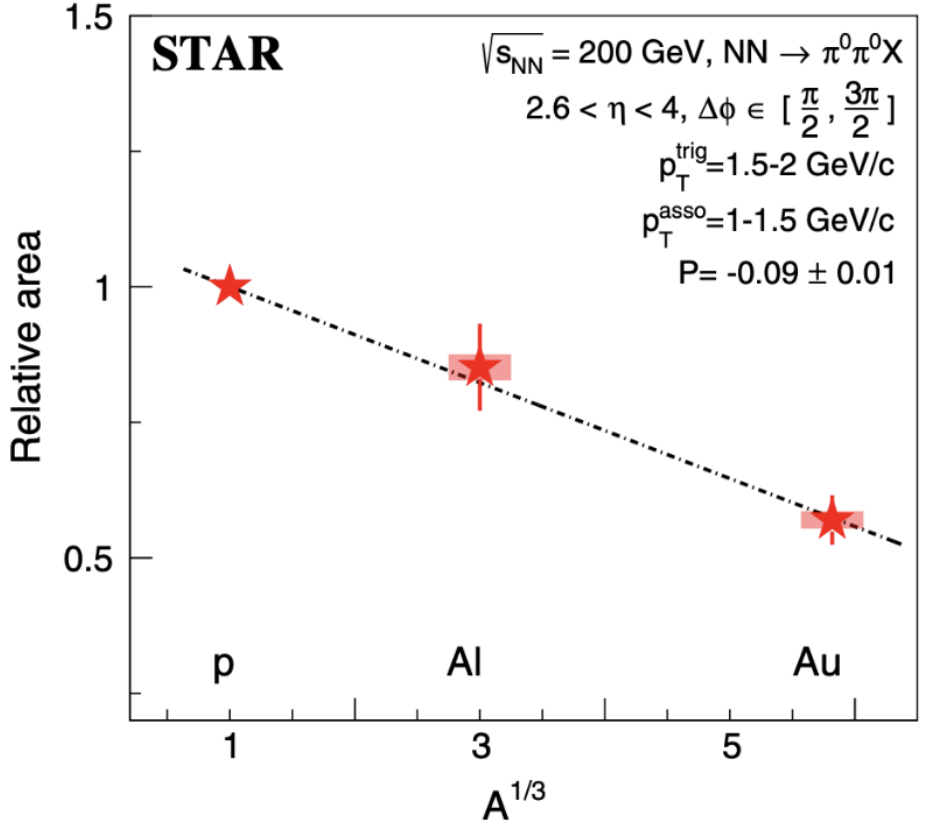

- At low p_T regime, a clear suppression is observed in p+A compared to the p+p data
- Such suppression scaling with $A^{1/3}$ matches gluon saturation models

Summary

- STAR measured the coherent and incoherent J/ψ production in Au+Au UPCs
- STAR observed the spin interference of the photoproduced ρ^0 and J/ψ
  - The measured interference signal increases with p_T
  - Measurements are sensitive to nuclear geometry and useful to constrain the theoretical models
- Baryon number carrier and its transport
  - Three approaches to test the carrier of baryon number & transport:
    - Isobar data: less electric-charge transport than baryon transport
    - Au+Au BES/global data: exponential rapidity dependence with slope showing no centrality dependence, flavor blind
    - Significant net-proton in γ+Au at midrapidity: exponential rapidity slope is compatible with the prediction of Regge theory on baryon junction
- First diffractive A_N is studied, but diffractive A_N can not have a significant contribution to large A_N
- STAR di-π^0 correlation study shows strong suppression at low p_T in p+A, following expected $A^{1/3}$ dependence

Backup slides

Results: characteristic features of γ+Au events

Model calculations:
Lewis et. al, arXiv: 2205.05685

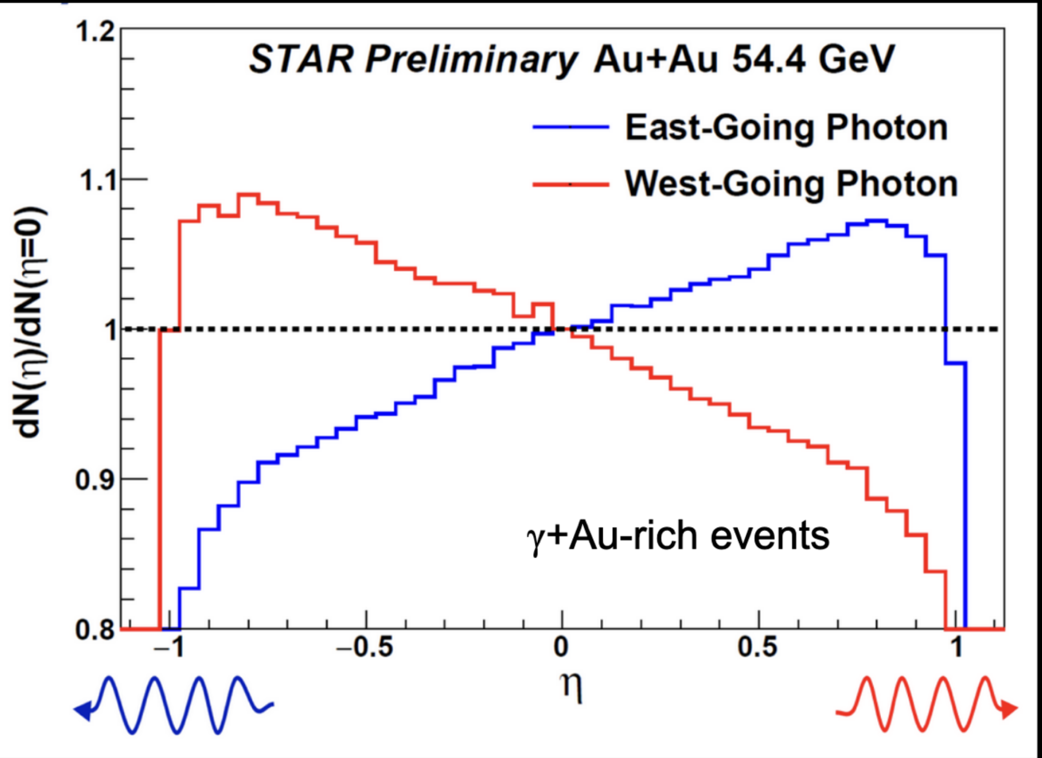

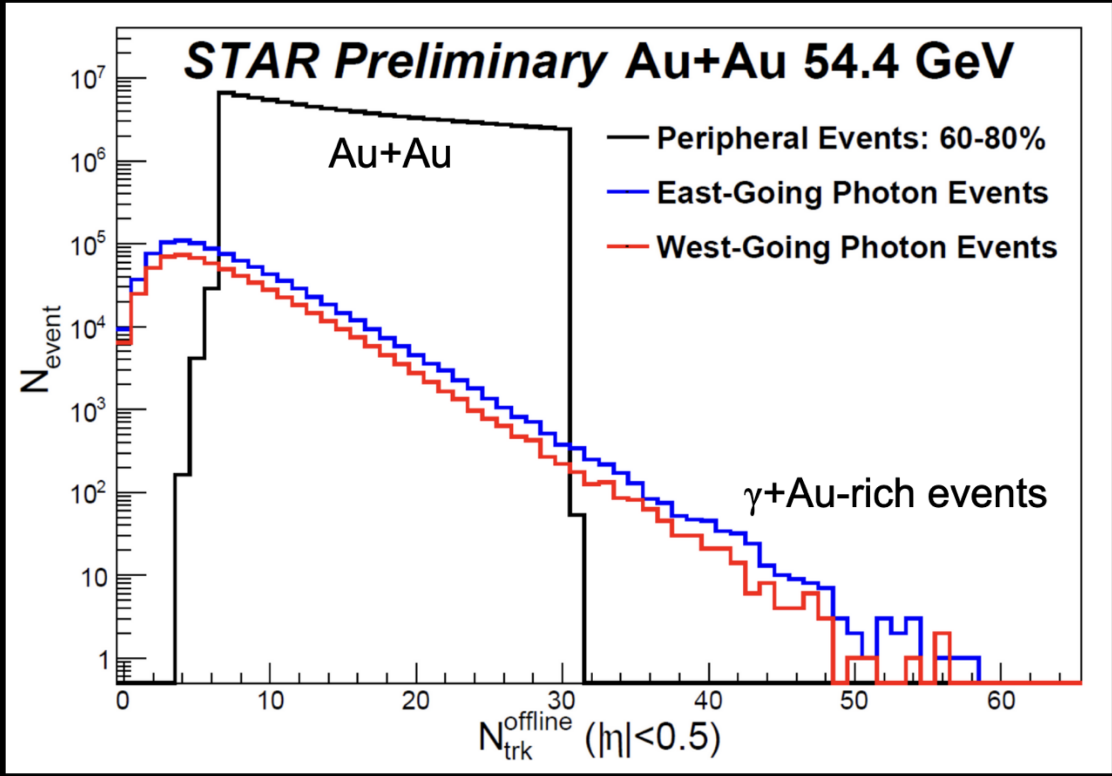

γ+Au events produce rapidity asymmetry that is expected from model predictions

Most photonuclear events have low multiplicity, consistent with very peripheral Au+Au collisions

Bulk features of γ+Au events are consistent with expectations from models

STAR forward upgrade

Coverage: $2.5 < \eta < 4.0$

Status:

- Installation and commission completed in 2021
- Start taking data since 2022

Requirements:

Detector	pp and pA	AA
ECal	$\sim$10 % / $\sqrt{E}$	$\sim$20 % / $\sqrt{E}$
HCal	$\sim$50 % / $\sqrt{E}$ + 10%	-
Tracking	Charge separation photon suppression	$\delta p_T/p_T$ $\sim$20 - 30% for $0.2 < p_T < 2$ GeV/c

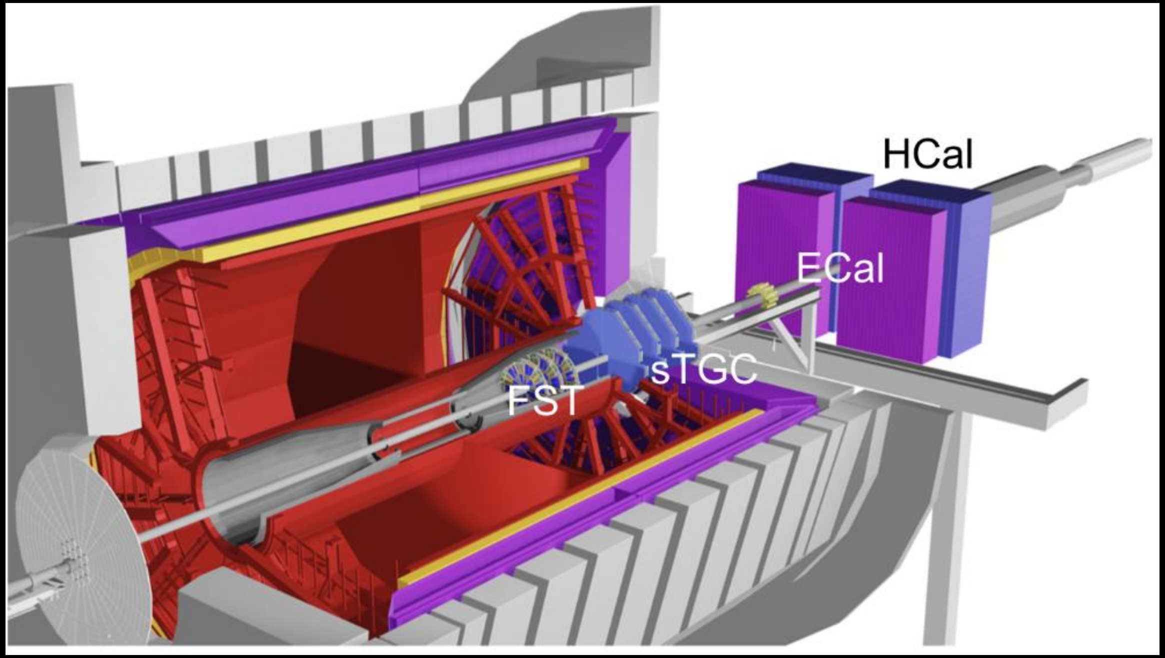

Measures:

- **$h^{+/-}$, $e^{+/-}$ (with good e/h separation)**
- **Photon, π^0, jets**

Combines:

- Forward Tracking System (FTS)
  - Forward Silicon Tracker (FST)
  - small-strip Thin Gap Chambers (sTGC)
- Forward Colorimeter System (FCS)
  - Electromagnetic Calorimeter (ECal)
  - Hadronic Ca**lorimeter (HCal)**

STAR: Forward tracking system (FTS)

Forward Tracking System (FTS):
- Forward Silicon Tracker (FST)
- small-strip Thin Gap Chambers (sTGC)

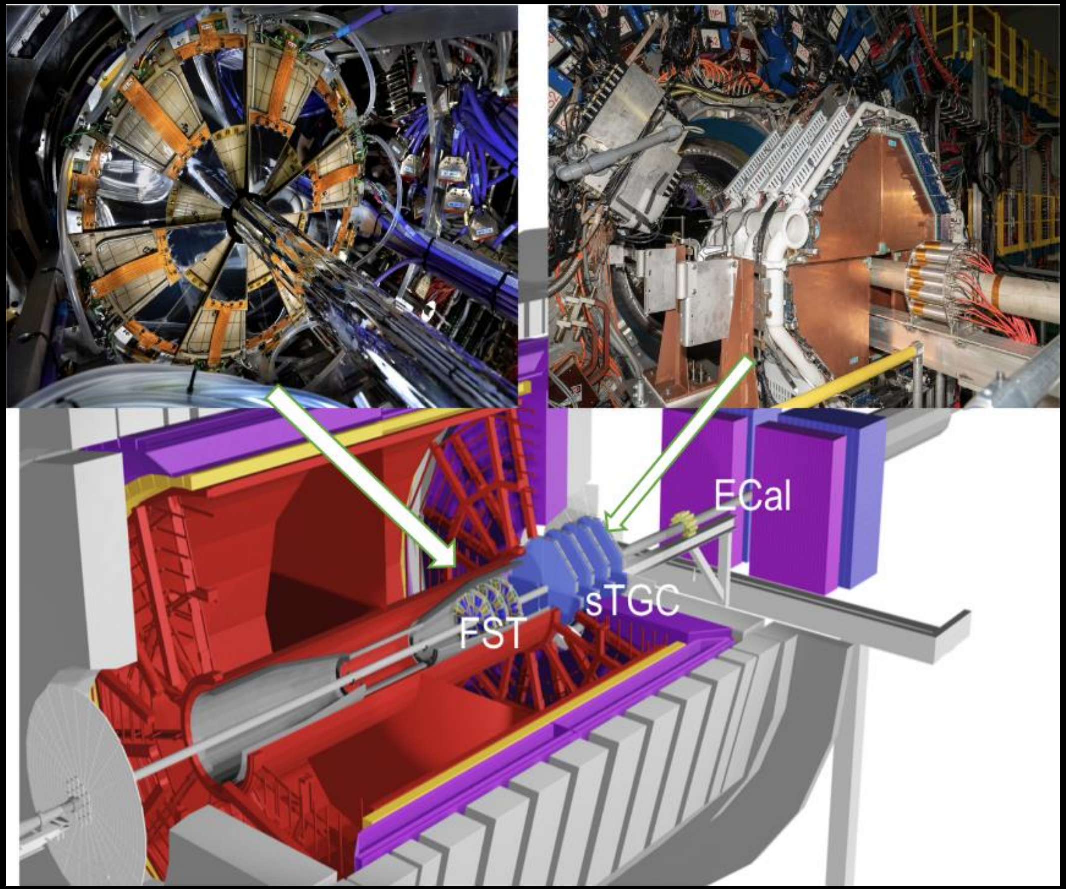

Forward Silicon Tracker (FST):
- 3 disks, each with 12 modules
- Each module includes 3 single-sided double-metal mini-strip sensors (Si from Hamamatsu)
  - Fine granularity in ϕ and coarse in R
  - Material **budget ~ 1.5% X_0 per disk**

small-strip Thin Gap Chambers (sTGC):
- 4 planes, each with 5 pentagonal modules
  - Double-sided sTGC with diagonal strips give x, y, u in each layer
  - Position resolution < 200 μm
- Material budget ~ 0.5% X_0 per layer
- Readout based on VMM chips

STAR: Forward calorimeter system (FCS)

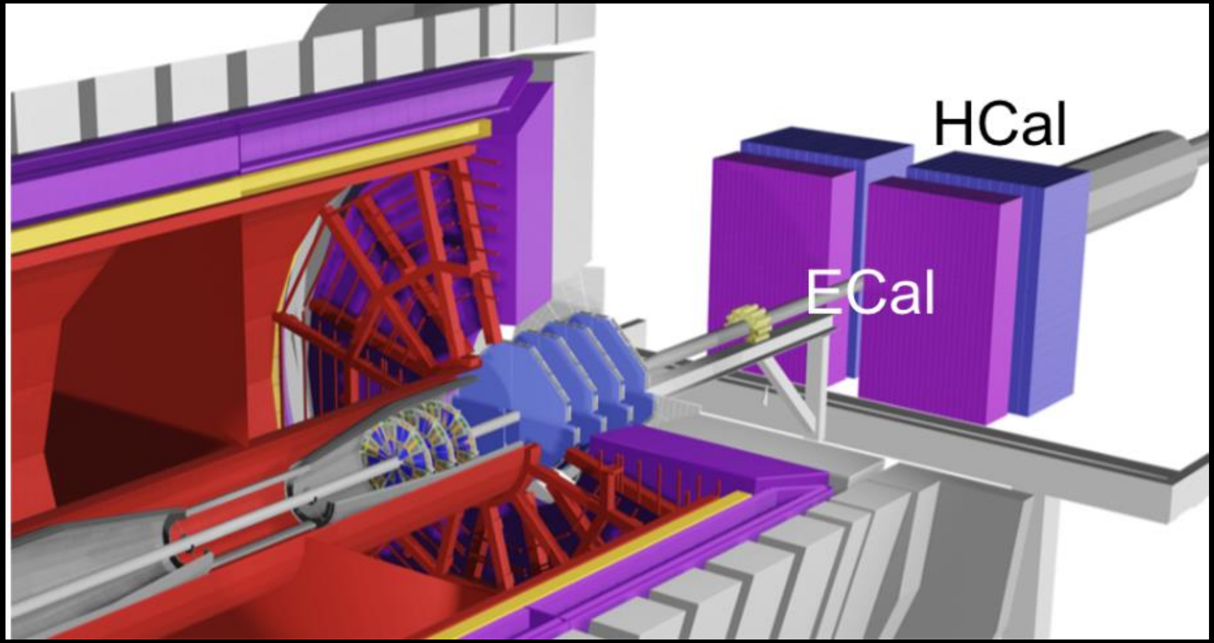

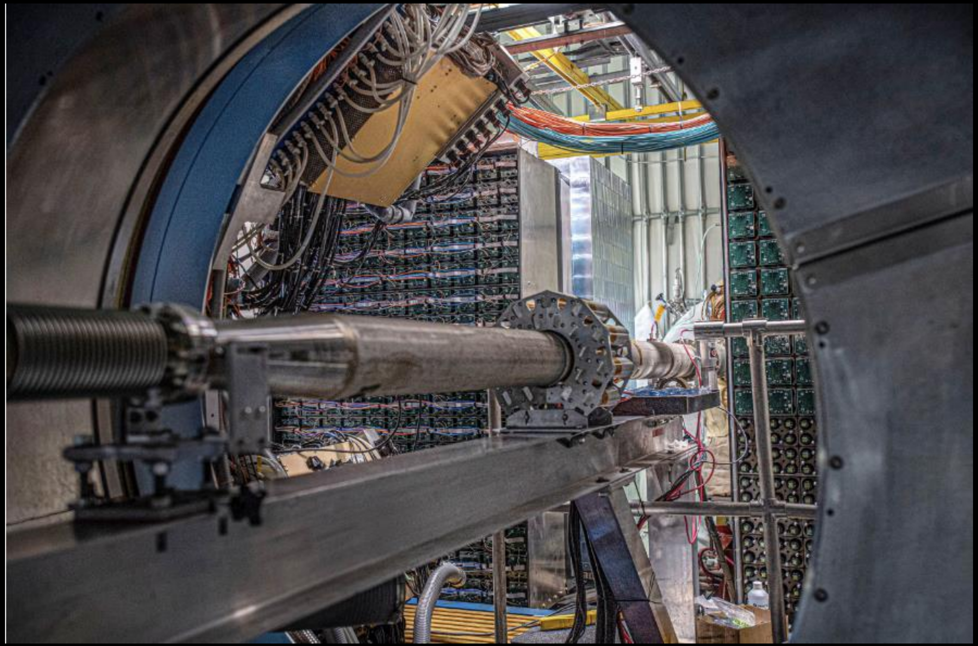

ECal:

- Reuse PHENIX Pb-Scintillator calorimeter
  - 1496 channels: $5.52 \times 5.52 \times 33\ cm^3$
  - 18 X_0; 0.85 nuclear interaction length
- SiPM readout

HCal:

- Fe/Sc (20 mm/3 mm) sandwich
  - 520 channels: $10 \times 10 \times 84\ cm^3$
  - $\sim$ 4.5 nuclear interaction length
- Same SiPM readout as ECal

Physics opportunities with the STAR forward upgrade

Cold QCD:

- Sivers asymmetries for hadrons, (tagged) jets, and di-jets
- Collins measurements at high x
- GPD E_g : gluon spin-orbit correlations
- Gluon PDFs for nuclei: R_{pA} for direct photons & DY
- Test of Saturation predictions through di-hadrons, γ-jets

Hot QCD:

- Temperature dependence of viscosity through flow harmonics up to $\eta \sim 4$
- Longitudinal decorrelation up to $\eta \sim 4$
- Global Lambda Polarization: test predictions of strong rapidity dependence

Physics opportunities with the STAR forward upgrade

PRL129, 092501 (2022)

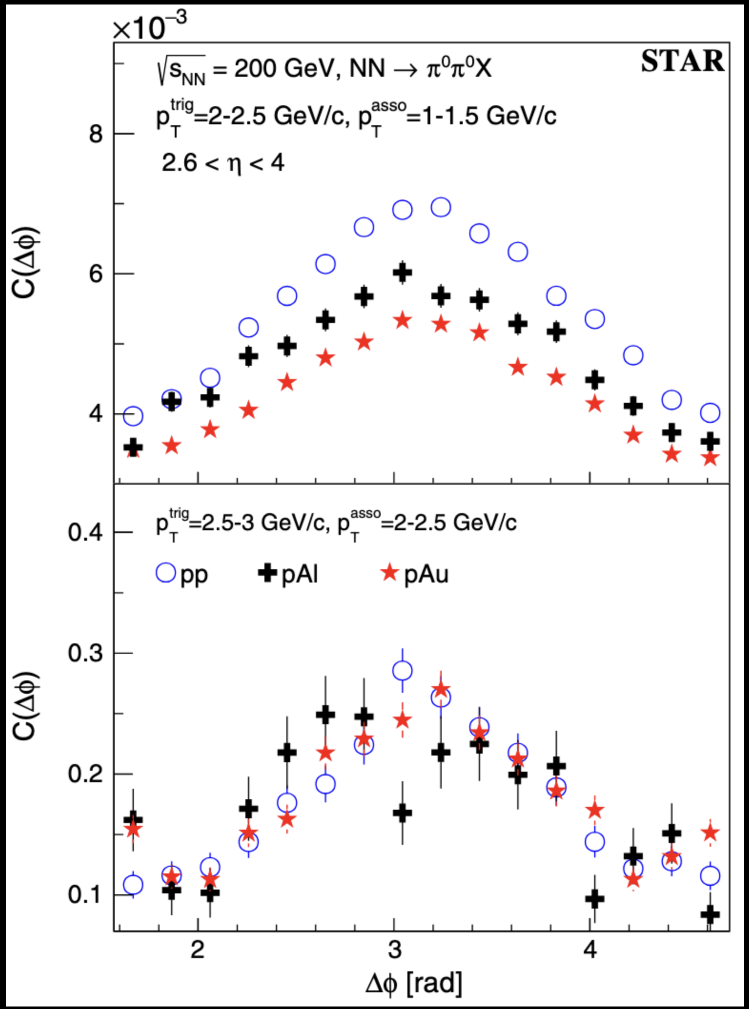

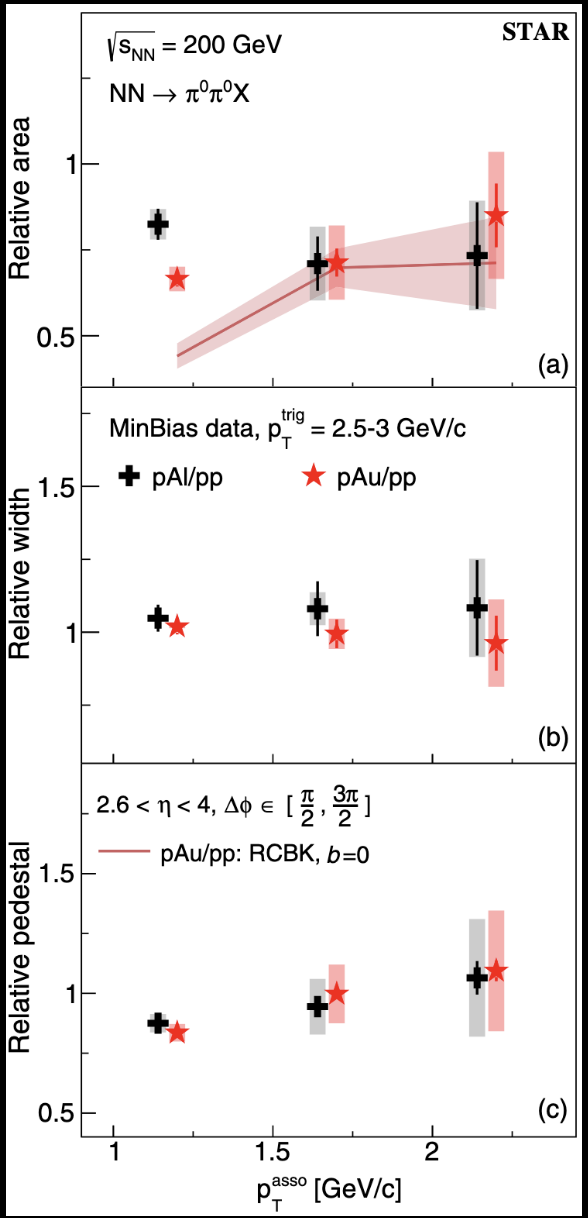

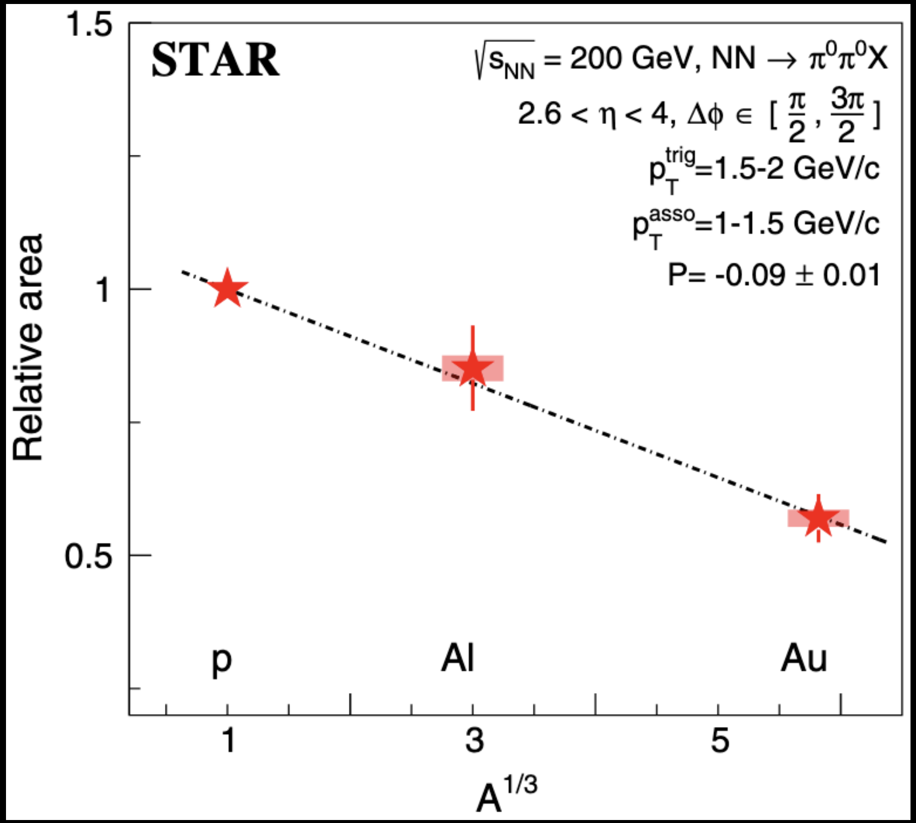

No increase in the width of the azimuthal angular correlation is seen within experimental uncertainties